UCRL-17372

University of California

Ernest O. Lawrence Radiation Laboratory

BROADBAND MODULATION OF HIGH-Q RESONATORS AT HIGH POWER LEVELS

TWO-WEEK LOAN COPY

This is a Library Circulating Copy which may be borrowed for two weeks. For a personal retention copy, call Tech. Info. Division, Ext. 5545

DISCLAIMER

This document was prepared as an account of work sponsored by the United States Government. While this document is believed to contain correct information, neither the United States Government nor any agency thereof, nor the Regents of the University of California, nor any of their employees, makes any warranty, express or implied, or assumes any legal responsibility for the accuracy, completeness, or usefulness of any information, apparatus, product, or process disclosed, or represents that its use would not infringe privately owned rights. Reference herein to any specific commercial product, process, or service by its trade name, trademark, manufacturer, or otherwise, does not necessarily constitute or imply its endorsement, recommendation, or favoring by the United States Government or any agency thereof, or the Regents of the University of California. The views and opinions of authors expressed herein do not necessarily state or reflect those of the United States Government or any agency thereof or the Regents of the University of California.

Research and Development

UCRL-17372
UC-28 Particle Accelerator
and High Energy Voltage
Machines

UNIVERSITY OF CALIFORNIA

Lawrence Radiation Laboratory
Berkeley, California

AEC Contract No. W-7405-eng-48

BROADBAND MODULATION OF HIGH-Q RESONATORS AT HIGH POWER LEVELS

Kenneth R. MacKenzie

February 23, 1967

BROADBAND MODULATION OF HIGH-Q-RESONATORS AT HIGH POWER LEVELS

Kenneth R. MacKenzie*

Department of Physics
University of California at Los Angeles
Los Angeles, California

February 23, 1967

ABSTRACT

Electronic broadband frequency modulation of a high-Q resonator operating at high voltage is considered. The simple overcoupled transformer is shown to be the most practical way to couple the final amplifier tubes to the resonator. Capacities other than the resonator capacity and the inherent tube capacity should be minimized. Transmission lines should be high-impedance and as short as possible. The maximum frequency range is shown to be governed by $V_1 \Delta\omega = 1.4\ \gamma g$, where V_1 is the resonator voltage, $\gamma = V_1/V_2$ (where V_2 is the tube rf voltage), and $g = I_e$ is the tube filament emission and C_2 is the tube capacity). This relation reduces to $V_2\ \Delta\omega = 1.4\ g$, showing that $\Delta\omega$ is limited only by tube parameters and not by resonator capacity or voltage. The minimum average power using a programmed dc plate voltage is shown to be $0.2\ V_1^2\ C_1\ \Delta\omega$ (where C_1 is the resonator capacity). Modulation rates, higher-order modes, transmission-line corrections, and other coupling schemes are discussed.

---

*This work was done for the Lawrence Radiation Laboratory, Berkeley, California.

INTRODUCTION

Most of today's large accelerators employ frequency modulation to keep electrode voltages in step with the circulating ions. Where the voltages are low, electronic methods using saturable ferrite are most practical. When the voltages are high and capacities are low, the ferrite method is still practical, but becomes progressively more difficult as capacities increase. In synchrocyclotrons the dee voltages and capacities are such that mechanical modulation is the obvious choice.

Recently there has been renewed interest in applying broadband electronic frequency modulation to the synchrocyclotrons. A successful step in this direction has been taken in the model studies for an FFAG accelerator, where a nominal frequency range of 32 to 23 Mc was covered.[1] A proposed extension of this method has been studied and reported[2] in which a range of almost 4 to 1 in frequency is covered in three steps. It has been pointed out in several recent reports that this method is applicable to cyclotrons. In one form or another, the suggestion is made to cut the D-shaped electrode into center-fed C-shaped pieces, each with a smaller capacity and smaller required frequency range.[3] Electronic modulation is certainly possible in this way. It remains to optimize the design in order to minimize the power, the number of electrodes, and the overall complexity.

Several laboratories are presently studying and modeling rf systems along these lines in the hope of replacing the mechanical rotary capacitors. It is therefore somewhat unfortunate that in spite of the current and future expense involved in research and development along these lines, and the large potential improvement in machine performance, the basic principles underlying the application of broadband modulation to accelerators is sparsely reported in the open literature. This is in sharp contrast to the numerous papers on magnetic-field studies. One reason lies in the mathematical complexity of any practical frequency-modulated rf system. Conventional methods of analysis lead immediately to cumbersome expressions which tend to hide the underlying physics or engineering.

In this paper some measure of visual insight is preserved through a pictorial analysis. The fundamental role of tube-filament emission is emphasized throughout. Some simple basic relations are derived for single- and double-tuned circuits when the frequency range is small, along with

---

1. E. M. Rowe, R. H. Hildon, R. F. Stump, and D. A. Swenson, Rev. Sci. Instr. 35, 1470 (1964).
2. F. T. Cole, G. Parzen, E. M. Rowe, S. C. Snowdon, K. R. MacKenzie, and B. T. Wright, Nucl. Instr. Methods 25, 189 (1964).
3. E. H. Molthen, Conference on High Energy Cyclotron Improvement, College of William and Mary, Feb. 6-8, 1964; W. M. Brobeck, Conference on High Energy Cyclotron Improvement, College of William and Mary, Feb. 6-8, 1964; S. Kullander, S. Holm, B. Johansson, and A. Tidricks, Synchrocyclotron Progress Report, Univ. of Uppsala, April 1, 1965 - Dec. 15, 1965.

exact relations which can be applied for wider ranges to special cases where transmission-line capacities can be neglected. Finally, transmission-line corrections are presented and a qualitative discussion is given on the importance of properly locating higher-order modes with respect to harmonics of the fundamental.

THE SIMPLE CIRCUIT

Emission Limitation

Some basic features of electronic modulation can be simply introduced (and noted for future use) by considering a tube in parallel with an LC circuit as shown in Fig. 1. (It should be some form of shield grid tube, or a triode in a grounded-grid circuit; although grounded-grid circuits offer problems when used with large driving power). C_1 is the capacity of the accelerating electrode, C_2 is the anode capacity to ground (internal and external), and C_e is the effective capacity introduced by the emission current. It may be positive, or it may be negative (which is equivalent to an inductance at any given frequency).

When the grid is driven at the natural resonant frequency $L_1(C_1+C_2)$, C_e will be zero, since the plate current pulses will flow exactly 180 deg out of phase with the plate rf voltage. At some other frequency, $\omega+\delta\omega$, well away from resonance, the relation

$$\omega + \delta\omega = L_1(C_1+C_2+C_e)^{-1/2} \tag{1}$$

must hold, where C_e is the capacity needed to make the system resonant at $\omega+\delta\omega$. The electron-emission current, which flows 90 deg out of phase with the plate rf voltage and gives the effect of this capacity, is given by $I_e = VC_e\omega$. It is seen at once that the voltage that can be developed off resonance is proportional to the available emission current.

As suggested by Fiebig,[4] the output voltage across C_1 can, in principle and practice, be held constant by a feedback link which controls the grid voltage as shown in Fig. 1. This condition can also be approached by connecting a resistor across C_1, with power absorption as the square of the voltage, but in the following analysis the presence of the feedback link is assumed and circuit losses are neglected.

If C_e is small compared with (C_1+C_2), then we can expand the square root in Eq. (1) and obtain a simple relation for the one-sided deviation $\delta\omega$:

$$\frac{\delta\omega}{\omega} = \frac{1}{2}\,\frac{C_e}{C_1+C_2} = \frac{1}{2}\,\frac{I_e}{V\omega}\,\frac{1}{C_1+C_2}\,. \tag{2}$$

With the total range

$$\Delta\omega = 2\delta\omega, \tag{3}$$

4. A. Fiebig, RF Broad-band Amplifiers for Driving Reactive Loads, CERN 64-27, MSC Div., June 1964.

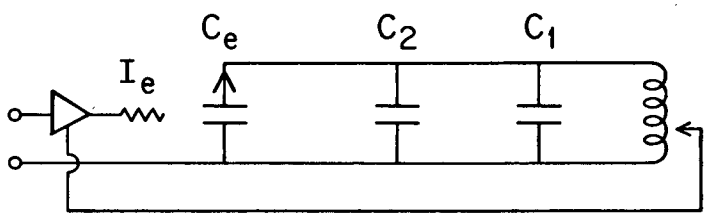

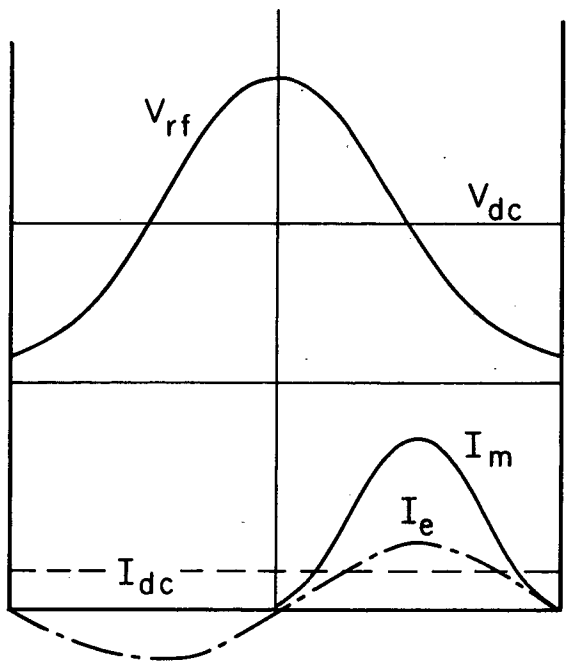

XBL672-954

Figs. 1 and 2

we can write this relation as

$$I_e = V(C_1 + C_2)\Delta\omega. \tag{4}$$

Tube manufacturers find it difficult to arbitrarily increase filament emission without increasing capacities, so we find in general that the available emission is proportional to the total anode-to-ground capacity C_2. If we write

$$I_e = g\,C_2, \tag{5}$$

the expression for the "voltage bandwidth" product is

$$V\Delta\omega = g\,C_2/(C_1 + C_2). \tag{6}$$

If we add a large number of tubes in parallel so that C_1 can be neglected, we have a limiting frequency range set by the inherent characteristics of the final amplifier tubes:

$$V\Delta\omega = g. \tag{7}$$

Usually, "g" is of the order of $1/2\times 10^{12}$ A/F.

Power Requirements

The emission limitation just discussed is fundamental. The power is a question of cost and cooling limitations.

If the voltage V in Eq. (4) represents the peak value, then the quantity I_e is the peak value of the fundamental component of the plate current. The in-phase fraction of the emission current can justifiably be neglected if we have a high-Q circuit and no parallel resistor. The emission current pulses will then flow 90 deg out of phase with the voltage as shown in Fig. 2.

The relations between the maximum emission current I_m, the peak value of the fundamental component I_e, the average value of the plate current I_{dc}, and the angle of flow θ, are given in Terman.[5] For an angle of 180 deg the peak value I_e is about 45% of I_m, and I_{dc} is about 27% of I_m. Since the in-phase component has been neglected, the pulses have symmetry about zero rf voltage and the plate power dissipation is simply $V_{dc}\,I_{dc}$. For typical conditions as shown in Fig. 2, V_{dc} is something like 1.2 V_{rf} and I_{dc} is about 0.6 I_e, which gives a power loss of roughly 3/4 $V_{rf}\,I_e$. If we use the value of I_e in Eq. (4) we find that approximate expression for the dc power dissipation at an interval $\delta\omega$ off resonance is

$$P \approx 1.5\,V_{rf}^{\;2}\,C\delta\omega, \tag{8}$$

where $C=C_1+C_2$, and the maximum value of $\delta\omega$ is given by Eq. (6).

5. Terman Electronic and Radio Engineering (McGraw Hill Book Co., Inc., New York, N. Y., 1955), 4th ed.

TWO COUPLED CIRCUITS

Inductive Coupling

In most situations, the arrangement shown in Fig. 1 is not practical. The modulating tube must be located some distance from the capacity C_1 and one must resort to some sort of coupling scheme. The simplest circuit, often referred to as an overcoupled transformer, is shown in Fig. 3. Its use as an element in a broadband system for accelerators has received considerable study.[6]

The two forms of inductive coupling shown in Fig. 3(a) and (b) differ only in the common connection between the two circuits. The form in Fig. 3(b) will be chosen for the following analysis. In practice, the circuits are often physically connected in just this manner. The inductances L_1, L_2, and M are usually short sections of transmission line, and their length permits the physical separation of C_1 and C_2.

The problem is simplified if one can neglect the transmission-line features. This is justified if the distributed capacity of the lines is small compared with C_1 and C_2 and if the lines are short. Fortunately this situation is often found in practice, and in these cases the sections of line can be approximated as inductances. Corrections for line effects are discussed later.

Identical Circuits

It is well known that the circuits in Fig. 3 have double-humped responses. If the individual circuits are separately tuned to two different frequencies f_1 and f_2, one normal mode of the system will be found close to f_1 and the other normal mode will be close to f_2. If the mode near f_1 is chosen, then it will be found that most of the energy is circulating in the individual circuit tuned to f_1, and very little energy will be found in the other. This is undesirable, since we wish to maintain a high voltage across C_1 in both modes. Therefore a reasonable first step (which also simplifies the analysis) is to use tight coupling to separate the modes, and to make both circuits identical. The latter assumption implies the choice of a modulating tube (or tubes) with total plate-to-ground capacity equal to C_1.

The phases and voltages in various parts of the coupled system are shown in Fig. 4. The combination of voltage distribution and circuit elements in one diagram is a pictorial device that has been useful to the author as an aid in analysis. Figure 4(a) shows the antisymmetric normal mode in which there must be zero voltage at the midpoint (and no voltage across M), since the individual circuits are identical. This is the higher-frequency mode designated by $\omega_h = (L\,C_1)^{-1/2}$.

Figure 4(b) shows the symmetric mode in which I_1 and I_2 flow in phase through M.

---

6. A. Suzini, Some Wide-band Quarter Wavelength Line Coupling Circuits, CERN 64-48, Synchrocyclotron Machine Division, Nov. 1964.

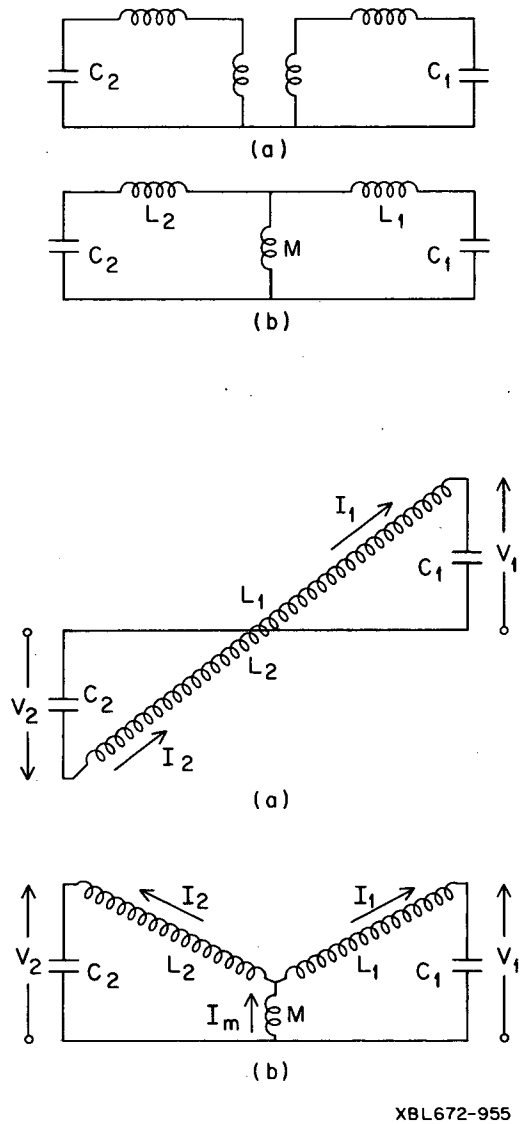
C2
C1
(a)
L2
L1
C2
M
C1
(b)
I1
C1
V1
L1
L2
V2
C2
I2
(a)
I2
I1
V2
C2
L2
L1
C1
V1
Im
M
(b)
XBL672-955

Figs. 3 and 4

If all the inductances are simple in shape, such as short transmission line sections, then the current streamlines, which never cross each other, are easily visualized. Current I_1 flows over part of the surface of M, and I_2 flows over the remainder. A cut can therefore be made parallel to the current streamlines, and therefore M can be split into two parts M_1 and M_2 which add in parallel to give M. Since the magnetic lines enclose M, the two circuits in this form, although disconnected, cannot be physically separated. However the mathematical division can always be performed regardless of shape, and values of M_1 and M_2 can be substituted which permit complete separation. Although separated, the points A and B in Fig. 5(a) are always at exactly the same potential. If the circuits are identical, we have $M_1 = M_2 = 2M$, and from Fig. 5(a) the lower symmetric mode frequency is seen to be

$$\omega_\ell = \{C_1(L+2M)\}^{-1/2}. \tag{9}$$

While the circuit is oscillating at this lower-mode frequency, let us raise the frequency of the grid driving voltage. The shield grid is assumed to be perfect and prevents any electrostatic coupling, so we have only the one-way coupling through the electron stream. As in the case of the simple circuit, we assume a feedback link which controls the grid voltage and sets the emission at the correct value to keep V_1 constant. The phase of the voltage V_2 automatically adjusts itself at 90 deg with respect to the emission current. This is a self-regulating property of any circuit which is driven off resonance.

Since the frequency has been increased, it is evident that the electron stream must look like an inductance and add a negative capacity to C_2 (negative capacities are shown dotted in the figure). This destroys the symmetry between circuits (1) and (2) and means that M_1 and M_2 must adjust themselves to make circuits (1) and (2) individually resonant at the new frequency. We note that M_1 must decrease to raise the frequency of circuit (1) and since we have

$$1/M_1 + 1/M_2 = 1/M, \tag{10}$$

it is evident that M_2 must increase. With points A and B at the same voltage, the autotransformer step-up ratios show at once that V_2 is now less than V_1:

$$\{M_1/(L+M_1)\}\, V_1 = \{M_2/(L+M_2)\}\, V_2. \tag{11}$$

The resonance condition is, with $C_2 = C_1$,

$$(C_1 - C_e)(L+M_2) = C_1(L+M_1) \tag{12}$$

or

$$C_e = C_1(M_2-M_1)/(L+M_2). \tag{13}$$

The capacities are related to the currents through

$$C_e = I_e/V_2\,\omega \tag{14}$$

and

$$C_1 = I_1/V_1\omega.$$

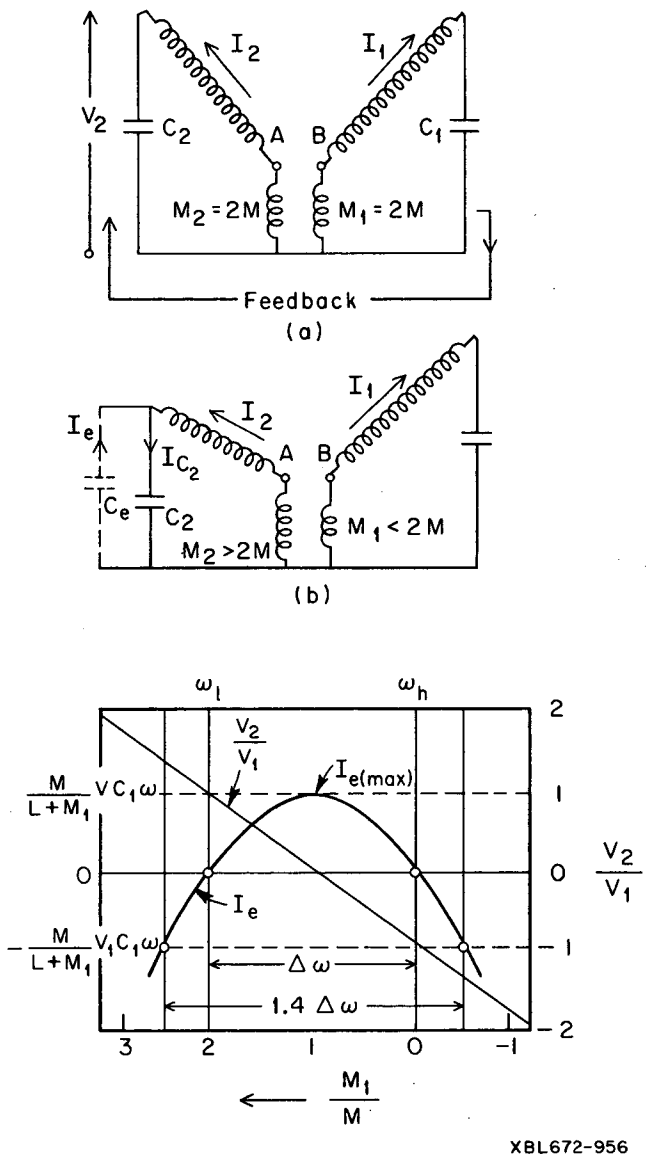
I2
I1
V2
C2
A
B
C1
M2 = 2M
M1 = 2M
Feedback
(a)
Ie
IC2
Ce
C2
M2 >2M
M1 < 2M
(b)
ωl
ωh
V2/V1
Ie(max)
M/(L+M1) VC1ω
0
Ie
M/(L+M1) V1C1ω
Δω
1.4 Δω
2
1
0
-1
-2
3
2
1
0
-1
M1/M
V2/V1
XBL672-956

Figs. 5 and 6

Combining Eqs. (10), (11), (13), and (14) we find

$$I_e = \frac{M_1}{M}\left(2 - \frac{M_1}{M}\right)\frac{M}{L+M_1} V_1 C_1 \omega . \tag{15}$$

If the frequency range is small, as it will be if high voltages are desired, then ω is approximately constant and $I_{e(max)}$ occurs approximately at $M_1 = M$. We then have $I_{e(max)} = [M/(L+M)] V_1 C_1 \omega$, or

$$[1+(M/L)] I_e = (M/L) V_1 C_1 \omega. \tag{16}$$

In Fig. 6 we have plotted I_e and V_2/V_1 vs M_1/M. We note that for $M_1 = 2M$ we have the lower mode ω_ℓ and for $M_1 = 0$, circuit (1) resonates at $\omega_h = (L\,C_1)^{-1/2}$. Therefore M_1/M represents a frequency scale.

The ratio M/L is related to the separation between modes through Eq. (9), which can be written (for $M/L \ll 1$)

$$\omega_\ell = \omega_h - \Delta\omega = \{C_1 L(1+2M/L)\}^{-1/2} \approx \omega_h(1-M/L), \tag{17a}$$

and we find

$$\Delta\omega/\omega \approx M/L. \tag{17b}$$

Combining this result with Eq. (16), we can write

$$I_{e(max)} = [1+(\Delta\omega/\omega)]^{-1} (M/L) V_1 C_1 \Delta\omega \approx V_1 C_1 \Delta\omega, \tag{18}$$

and with $I_e = gC_2$, and $C_2 = C_1$:

$$V_1 \Delta\omega = [1+(\Delta\omega/\omega)]\, g \approx g. \tag{19a}$$

A comparison of Eqs. (18) and (19) with Eqs. (4) and (6) shows that for a given voltage and frequency range the double-tuned circuit requires less emission (or allows a greater frequency shift $\Delta\omega$) in approximately the ratio $C_1/(C_1+C_2)$. The reason is that $V_2 = 0$ when I_e is a maximum and there is no energy stored in the tube capacity C_2. Moreover, the shift $\Delta\omega$ in Eq. (6) is the maximum possible shift; whereas the shift $\Delta\omega$ in Eq. (19) refers only to the separation between modes. Extra range can be added above and below the mode frequencies. If we suppose that we have an emission limit determined from Eq. (18) then we seen from Fig. 6 that this same current, with opposite phase, is found when the frequency range is 1.4 $\Delta\omega$. The coupled circuit with identical LC elements is therefore able to cover a considerably wider range $\Delta\omega$ than the single circuit. We find

$$\Delta f(\text{coupled})/\Delta f\,(\text{single}) \approx \sqrt{2}\,(C_1+C_2)/C_1. \tag{19b}$$

However, we note from Fig. 6 that the tube voltage $V_2 = \pm 1.4\, V_1$ at the extremes. When we discuss power requirements, we will see that a rather high price must be paid for these extra portions of the possible frequency range.

The above relations have been obtained with the restriction that $M_1 << L$, which is almost equivalent to saying that $M << L$, or that $\Delta\omega/\omega << 1$. If this is not the case, the exact relation in Eq. (12), with $\omega = \{C_1(L+M_1)\}^{-1/2}$, should be plotted for chosen values of M/L.

A Step-by-Step Pictorial Review

It is instructive, and also useful for later reference, to show pictorially the voltage distributions at several frequencies throughout the range $\Delta\omega$. The sequence starts with the lower mode frequency ω_ℓ shown in Fig. 5(a), where the tube voltage V_2 is equal to the electrode voltage V_1. Figure 5(b) shows a somewhat higher frequency, where C_e has been substracted from C_2. Figure 7(a) shows a still higher frequency, where $M_1 = M$ and M_2 must be infinite [see Eq. (10)]. This means that no current can flow through L in circuit (2), which in turn implies that there can be no voltage drop along L. V_2 is therefore equal to the voltage across M (denoted by V_m). This condition is found when the inductance represented by the emission current resonates with C_2, or when $C_2 - C_e$ is zero (which is the same thing). At this frequency, which we will call ω_m, the emission current is merely charging the tube capacity to $V_2 = V_m$. Therefore we have

$$I_e = V_2 C_2 \omega_m = [M/(L+M)]\ V_1 C_1 \omega_m. \tag{20}$$

At a slightly higher frequency we must have $M_1 < M$, which means that M_2 is negative and physically corresponds to a capacity. This is shown in Fig. 7(b). The current through L in circuit (2) must now be in the reverse direction, and at the same time this current will produce a voltage drop such that V_2 is less than the voltage across M. The tube looks like an inductance. As the frequency is again raised very slightly, we have the picture in Fig. 7(c). The mutual element $(-M_2)$ resonates with L, and the tube voltage is zero, corresponding to zero inductance. This is the condition for series resonance and occurs at a frequency that we will call ω_s.

At this frequency, the diagram is easier to analyze if we do not split M into a parallel combination of capacity and inductance, so Fig. 7(c) has been redrawn as shown in Fig. 7(d). The relations between voltages and currents are:

$$I_e + I_m = I_1 = V_1 C_1 \omega_s$$

and

$$I_e / I_m = M/L,$$

and we find

$$I_e = [M/(L+M)]\ I_1 = [M/(L+M)]\ V_1 C_1 \omega_s. \tag{21}$$

This relation is the same as Eq. (20), and we see that the emission current at series resonance exceeds I_e at ω_m by the ratio ω_s/ω_m. Equation (21) is the same as Eq. (16) and with $\Delta\omega/\omega = M/L$, $C_1 = C_2$, and $I_e = gC_2$ we find the result in Eq. (19), namely $V\Delta\omega = [1+(\Delta\omega/\omega)]\,g$.

Figure 8(a) shows what happens as we move to a frequency slightly above ω_s. The electron emission current continues to flow in the same

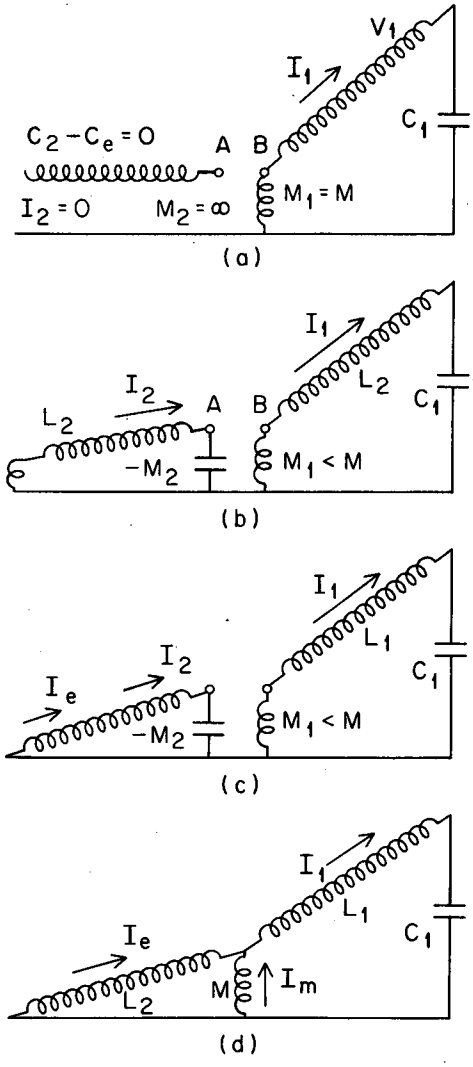

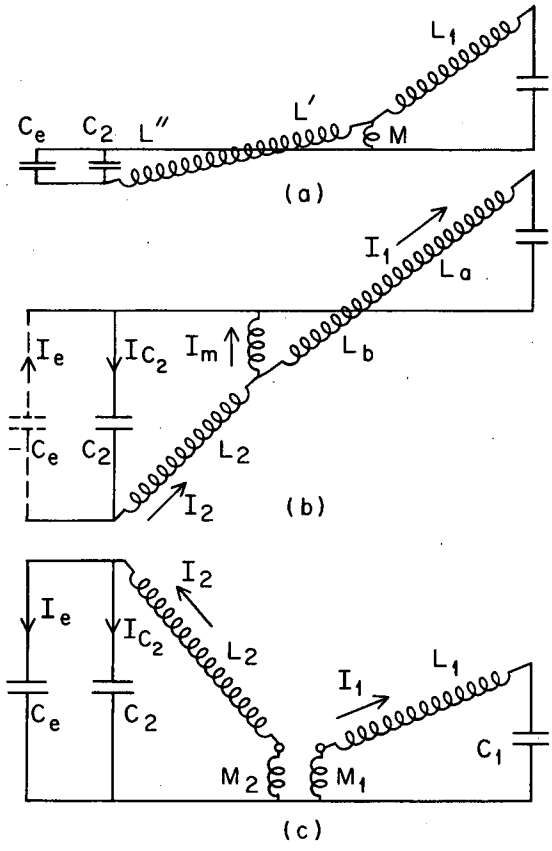

XBL672-957

Figs. 7 and 8

sense (which is in phase with I_1). However, the voltage across the tube reverses, so the emission current creates a huge capacity which adds to C_2. Anode appears somewhere along L, which we then divide into L' and L''. The hugh capacity $C_e + C_2$ resonates with L'' in Fig. 8(a), while L' adds in parallel with M to make circuit (1) resonate at the same frequency.

Figure 8(b) shows what happens when the frequency is above ω_h. The reduced inductance in circuit (1) is denoted by L_a, and we have $L_a + L_b = L$. The inductance in circuit (2) is now greater than L, so the emission current subtracts the appropriate capacity C_e to make things right. It is evident by inspection that $V_2 > V_1$ and opposite in phase, (as also indicated in Fig. 6). To complete the sequence, Fig. 8(c) shows the distribution at a frequency below ω_ℓ. Again we note that V_2 is greater than V_1.

Figure 9 shows the reactance presented by $C_2 - C_e$ plotted against frequency. We note that it is the ability of the electronic reactance to go continuously through infinity at ω_m and zero at ω_s (where $V_2 = 0$) that makes it possible to pass smoothly from the symmetric to the antisymmetric mode. If the amplifier tube were to be replaced by a mechanical variable capacitor, only the portions of the curve to the left of ω_m or to the right of ω_s would be available. Mode transfer would not occur. In practice this is no serious disadvantage, since the mechanical device is not emission-limited, and therefore the range can be extended far above ω_h or far below ω_ℓ. The limitation becomes voltage breakdown, since the voltage rises in either direction.

Nonidentical Circuits

In our previous example, the symmetry made $V_2 = V_1$ at ω_ℓ and ω_h. In the region between ω_ℓ and ω_h, we observed that the rf voltage V_2 was always less than V_1 and actually dropped to zero at series resonance (neglecting losses). As the voltage decreases, the ratio of the available electron-emission current to the tube-reactive current increases, since the former remains constant. This suggests that if the voltage across the tube, V_2, were to be lowered at all frequencies, the filament emission current would be proportionately more effective.

By inspection of Fig. 5(b) we see that subtracting capacity from C_2 lowers V_2 in the symmetric mode, but Fig. 8(b) shows that V_2 is raised in the corresponding antisymmetric mode. This general property is worth noting and is useful for empirical tuning, but we would like a modification that lowers V_2 in both modes. We now search for a corresponding change in L_2 that will produce the desired effect. Figure 10 shows a circuit in which L_2 and C_2 are related to L and C through the parameters α and β which we will determine, subject to the condition that $V_1 V_2 = \pm\gamma$ where $|\gamma| > 1$.

In the symmetric mode M_1 and M_2 are denoted by M_1^s and M_2^s respectively. In the antisymmetric mode, they are denoted by M_1^a and M_2^a (M_1^a turns out to be negative in this mode, corresponding to an inductance, and M_2^a is less than M). In circuit (2) of Fig. 10, we have increased C_2 and decreased L_2 by setting $C_2 = \alpha C$ and $L_2 = L/\beta$. If we set $V_1/V_2 = \gamma$ in the symmetric mode and $-\gamma$ in the other mode we have:

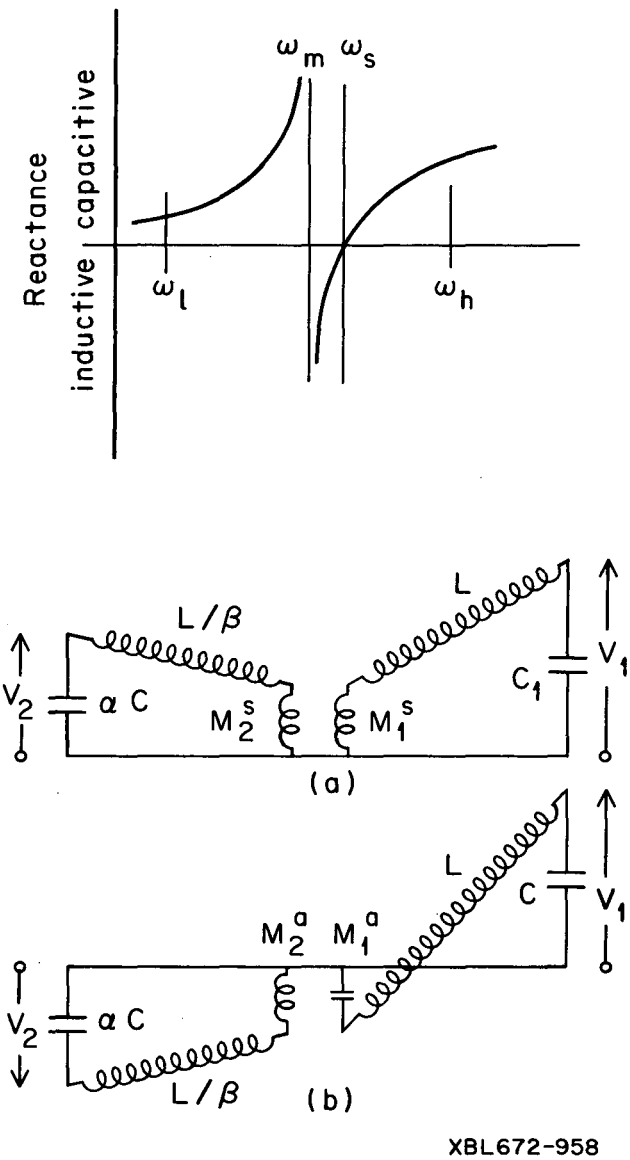
Reactance
capacitive
inductive
ω_m
ω_s
ω_l
ω_h
L/β
L
V_2
α C
M_2^s
M_1^s
C_1
V_1
(a)
L
C
V_1
M_2^a
M_1^a
V_2
α C
L/β
(b)
XBL672-958

Figs. 9 and 10

$$\alpha C_1(M_2^{\,s} + L/\beta) = C_1(M_1^{\,s} + L) = 1/\omega_\ell^{\,2}, \tag{22}$$

$$\alpha C_1(M_2^{\,a} + L/\beta) = C_1(M_2^{\,s} + L) = 1/\omega_h^{\,2}, \tag{23}$$

$$\frac{M_2^{\,s}}{M_2^{\,s}+L/\beta}\,\frac{M_1^{\,s}+L}{M_1^{\,s}} = \gamma; \quad \frac{M_2^{\,a}}{M_2^{\,a}+L/\beta}\,\frac{M_1^{\,a}+L}{M_1^{\,a}} = -\gamma, \tag{24}$$

and

$$1/M_1^{\,s} + 1/M_2^{\,s} = 1/M_1^{\,a} + 1/M_2^{\,a} = 1/M. \tag{25}$$

These equations determine immediately that

$$\alpha = \gamma^2. \tag{26}$$

Solving for M_1, M_2, and M we obtain:

$$M_1^{\,a} = -\frac{(1-\gamma^2/\beta)}{\gamma+1}\,L, \qquad M_2^{\,a} = \frac{(1-\gamma^2/\beta)}{\gamma(\gamma+1)}\,L \tag{27}$$

$$M_1^{\,s} = \frac{(1-\gamma^2/\beta)}{\gamma-1}\,L, \qquad M_2^{\,s} = \frac{(1-\gamma^2/\beta)}{\gamma(\gamma-1)}\,L \tag{28}$$

$$M = \frac{(1-\gamma^2/\beta)}{\gamma^2-1}\,L. \tag{29}$$

In these formulae, L is some given inductance and γ is the voltage ratio we desire, so the only variable is β. The largest value of M, and therefore the largest frequency shift occurs when $\beta = \infty$ (corresponding to $L_2 = L/\beta = 0$). The minimum occurs when $\beta = \gamma^2$, where all mutual elements are zero and there is no coupling. If we have $\beta < \gamma^2$, then M is negative, corresponding to capacitive coupling, this will be discussed shortly.

At series resonance we have the diagram in Fig. 11, and as given in Eq. (21).

$$I_e = \frac{M}{M+L/\beta}\,I_1 .$$

Using the value of M from Eq. (29) we have

$$I_e = \frac{\beta-\gamma^2}{\beta-1}\,I_1 = \frac{\beta-\gamma^2}{\beta-1}\,V_1 C_1 \omega. \tag{30}$$

The frequency shift is given by $\omega_h/\omega_\ell = 1 + (\Delta\omega/\omega)$. From Eqs. (22) and (33) we write

$$\omega_h/\omega_\ell = [C(L+M_1^{\,s})/C(L+M_1^{\,a})]^{1/2}.$$

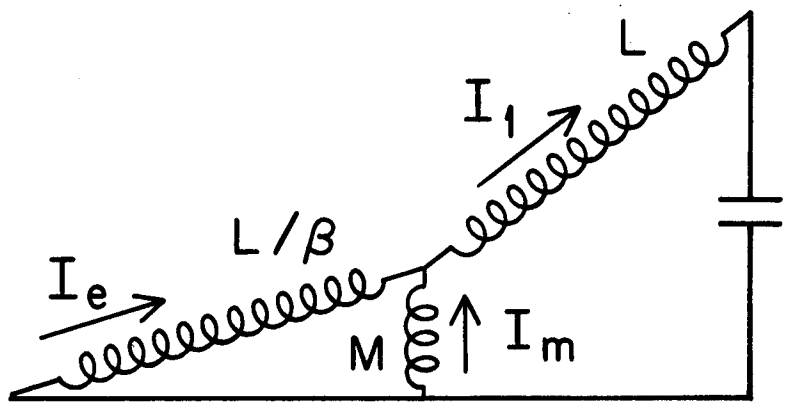

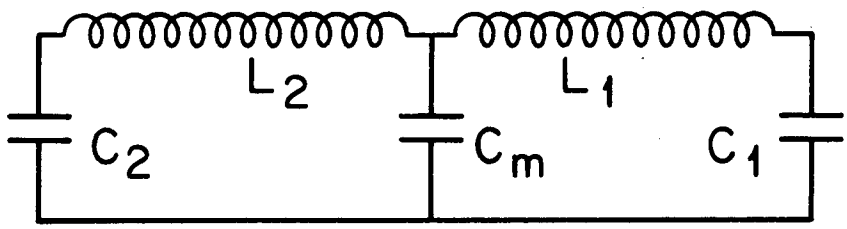

XBL672-959

Figs. 11 and 12

Inserting M_1^s and M_1^a from Eqs. (27) and (28) we have

$$\omega_h/\omega_\ell = \left(\frac{\gamma + 1}{\gamma - 1} \; \frac{\beta - \gamma}{\beta + \gamma}\right)^{1/2} . \tag{31}$$

If we let $\beta = \gamma^2 + \delta$, we can expand in terms of $\delta/\gamma(\gamma-1)$ and $\delta/\gamma(\gamma+1)$ and obtain

$$\omega_h/\omega_\ell = 1 + [\Delta\omega/\omega] = 1 + [\delta/\gamma(\gamma^2 - 1)],$$

and we see that

$$\Delta\omega/\omega = \frac{\beta - \gamma^2}{\gamma(\gamma^2 - 1)} . \tag{32}$$

For small frequency shifts, β will be somewhat greater than γ^2. For $\gamma \gg 1$ (e.g., 2 or 3), we can consider the denominator of Eq. (32) and put $(\gamma^2-1) = (\beta - 1)$ with very little error. The right-hand side of (32) is then γ times the result in Eq. (30), with the result that we have

$$I_e = \gamma(\Delta\omega/\omega)\, I_1 = \gamma\, V_1 C_1 \Delta\omega. \tag{33}$$

By comparison with Eq. (18), where $I_e = V_1 C_1 \Delta\omega$, Eq. (33) shows that the emission current must be increased over the identical-circuit case by the factor γ. But we also note from Eq. (26) that $\alpha = \gamma^2$, so $C_2 = \gamma^2 C_1$ and we have more than enough emission available. (For example, if $\gamma = 2$, then from Eq. (33), the nonidentical-circuit case requires twice as much emission as the identical-circuit case. But with $C_2 = \gamma^2 C_1 = 4C_1$, we can put four tubes in parallel and have four times the original emission available). Obviously this extra available emission should be used to obtain increased frequency range, and in general it would be some sort of sacrifice to simply add inert capacity to C_2 in order to produce the voltage ratio γ. Letting $C_2 = \alpha C_1 = \gamma^2 C_1$ and $I_e = g\, C_2 = g\, \gamma^2 C_1$, we rewrite Eq. (33) as

$$I_e = g\, \gamma^2 C_1 = \gamma\, V_1 C_1 \Delta\omega,$$

and obtain a final simple relation for the "voltage bandwidth" product when $\Delta\omega/\omega \ll 1$:

$$V_1 \Delta\omega = \gamma g, \tag{34}$$

or, since $\gamma = V_1/V_2$:

$$V_2 \Delta\omega = g. \tag{35}$$

This result immediately suggests that γ should be as large as possible. But obviously we cannot let γ approach ∞, since the frequency shift would go to zero. This is shown in Eq. (32), where we should keep in mind that β must always be greater than γ^2 to maintain inductive coupling (i.e., M must be positive).

Some of the above equations can be used in a cut and try self-consistent manner when $\Delta\omega/\omega$ is not small. For example, let us suppose that a given value of ω_h/ω_ℓ is desired. The application probably spells out some minimum separation between C_1 and C_2, which in turn specifies some minimum value for L_2 and therefore some maximum value for β. Using these values for β and ω_h/ω_ℓ, we solve for γ from Eq. (31).

Since we have $C_2 = \gamma^2 C_1$ we know how many tubes to put in parallel in circuit (2) and since we have $I_e = g\,C_2$, we know how much emission we have to work with. Finally we put this value of emission current in Eq. (30) along with the values of β and γ and determine the voltage V_1 that can be produced. If the calculated value of V_1 turns out to be the desired electrode voltage, then the problem is solved. If it turns out to be greater than needed, then there is bandwidth to spare, and β can be increased to provide more convenient separation between C_1 and C_2. If V_1 turns out to be too low, then there is no solution unless tubes with a larger g factor can be found.

It is probably worth noting that this cut-and-try method (which is not very tedious) is exact even for large frequency shifts in the limit where transmission-line effects can be neglected. Some approximate correction factors for line effects will be considered later.

Capacitive Coupling

For $\beta < \gamma^2$ we saw from Eqs. (27), (28), and (29) that M and all but one of its partitioned components become negative, corresponding to capacities. Capacitive coupling of circuits (1) and (2) is shown in Fig. 12. The symmetric and antisymmetric modes are shown in Fig. 13. By contrast with inductive coupling, the symmetric mode now oscillates at the higher frequency, and points of zero potential, or nodes, are found somewhere along the inductance L in each circuit.

The mutual element C_m can be split into two parallel capacities so that

$$C_m = C_a + C_b.$$

In this case we observe that the two circuits can immediately be physically separated in the symmetric mode and will oscillate at the same frequency. The resonance conduction is

$$\frac{1}{\omega^2} = L_2\left(\frac{C_2 C_b}{C_2+C_b}\right) = L_1\left(\frac{C_1 C_a}{C_1+C_a}\right). \tag{36}$$

Two values for C_a and C_b are found corresponding to the symmetric and antisymmetric modes. Unless the circuits are identical, one of the values of C_a or C_b will be negative, corresponding to an inductance. If the circuits are identical, we find $C_a = C_b = 1/2\,C_m$. For $C_m \gg C_1$, we find

$$\omega_\ell = (L\,C_1)^{-1/2};$$

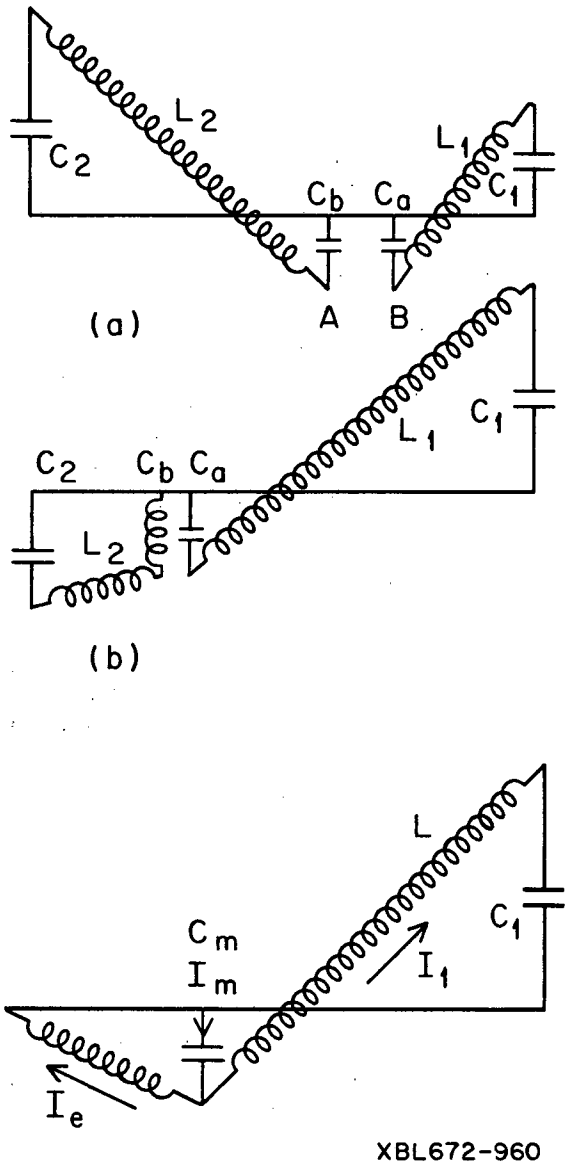

Figs. 13 and 14

and

$$\omega_h = [L C_1 \tfrac{1}{2} C_m/(C_1 + \tfrac{1}{2} C_m)]^{-1/2}$$
$$= \omega_\ell [1 + (C_1/C_m)],$$

and we have

$$\Delta\omega/\omega \approx C_1/C_m. \tag{37}$$

At series resonance V_2 is zero, and, as shown in Fig. 14, we have $I_e + I_1 = I_m$ and $I_e/I_m = (1/\omega C_m)/L\omega = 1/L\omega^2 C_m$. When these relations are combined, we find $I_e = I_1/(L\omega^2 C_m - 1)$. Letting $\omega^2 \approx 1/L C_1$, we find

$$(1 - C_1/C_m) I_e = (C_1/C_m) I_1 = (C_1/C_m) V C_1 \omega \tag{38}$$

If we substitute $\Delta\omega/\omega$ for C_1/C_m from Eq. (37) and $I_e = g C_1$, since $C_1 = C_2$ we have

$$V_1 \Delta\omega = [1 - (\Delta\omega/\omega] g \tag{39}$$

Comparing this relation with Eq. (19) where we have $V_1 \Delta\omega = (1 + \Delta\omega/\omega) g$, we see that in comparison with inductive coupling, capacitive coupling yields a slightly reduced range, or alternatively more filament emission is required. This is to be intuitively expected, since the mutual capacity stores charge, and some of the electron emission is diverted for this purpose.

In certain cases the capacitive-coupling scheme may have advantages. For mechanical simplicity it may be desirable to continue the transmission line from C_1 straight through a vacuum insulator to C_2. The constriction at the insulator can easily be augmented and made to serve as the capacitor C_m. The absence of a connection to ground also makes it easy to quench rf discharges with a dc bias on C_1. Except for this slight decrease in frequency range, this circuit behaves in general like its inductively coupled counterpart. Nonidentical circuits can be used to obtain different voltage ratios and extend the range.

Power Considerations

If we assume, for the case of identical circuits, that the plate-current pulses flow for half a cycle, then, as we saw earlier, the dc plate voltage should be about 1.2 times the peak rf voltage. If the dc plate voltage is constant, then the power can be directly found from Fig. 6 with $I_{dc} \approx 0.6 I_e$. If only the range $\Delta\omega$ is employed, the maximum power occurs at series resonance, ω_s, and is given by

$$P = (1.2 V_{rf})(0.6 I_e).$$

Using the value of I_e from Eq. (18), we have

$$P \approx (3/4)\, V_{rf}^{\,2}\, C_1\, \Delta\omega, \tag{40}$$

where $\Delta\omega$ between modes is found from Eq. (19); namely $V\Delta\omega \approx g$. If we compare this relation with Eq. (8), we see that the power required at series resonance (when the frequency shift is $\Delta\omega$ between modes) is $1/2\, C_1/(C_1+C_2)$ times the power required for a shift $\Delta\omega$ in a single circuit ($\Delta\omega = 2\delta\omega$, where $\delta\omega$ is the one-sided shift). The reason is as we mentioned earlier, simply, that no energy is stored in C_2 at the series resonance frequency ω_s, where $V_2 = 0$.

If the full possible range of the double-tuned circuit, $1.4\,\Delta\omega$, is used, then V_{dc} must be increased in the same ratio, as shown in Fig. 6. Since $I_{e(max)}$ is a constant, the power at the extremes is also increased in the same ratio. If the dc plate voltage is maintained constant at this elevated value throughout the range, the power is also increased by 1.4 at ω_s. This is a rather high price to pay for the extra range in view of the following saving that can be made within the range.

Figure 6 shows that V_2 decreases within the range $\Delta\omega$ and falls to zero at ω_s. Since V_{dc} needs only exceed $V_{(rf\ peak)}$ by $V_{min} \approx 2$ to 3 kV in most high-power tubes, the power-supply voltage can be reduced in appropriate fashion by a series modulator tube. The dissipation in the amplifier tube at ω_s thus becomes

$$P = V_{min}\, I_{dc} = V_{min}(0.6\, I_e) \approx 0.6\, V_{min}\, V_1 C_1\, \Delta\omega, \tag{41}$$

where V_1 is the peak rf voltage across capacitor C_1, and $\Delta\omega$, the frequency range between modes given by Eq. (19), is governed by the tube factor g. If V_1/V_2 is increased by γ, $\Delta\omega$ is increased accordingly and the power at series increases in the same ratio. No power saving results from the reduction in V_2 by $1/\gamma$, since I_e increases in inverse proportion [see Eq. (32)].

If the tube operates at about 15 kV at ω_h and ω_ℓ, and if V_{min} is about 3 kV, we have reduced the power by a factor of 5. However, the cost of power has not changed, since the remainder is lost in the modulator tube. Suzini points out that a simple series resistor would automatically drop the voltage in approximately the desired manner and suggests a natural extension to an LC circuit resonant at the fm repetition rate.[6] A slight variation of his circuit is shown in Fig. 15(a).

Figure 5(b) shows the dc sinusoidal output fitted to the variation in V_2. (It is assumed here that the frequency program is sawtooth in form as shown in Fig. 16). The current pulse I_e would drive this circuit as a low-frequency class-B amplifier.

However, no saving is made because the stored energy is lost in R. A means of recovering this energy is discussed later.

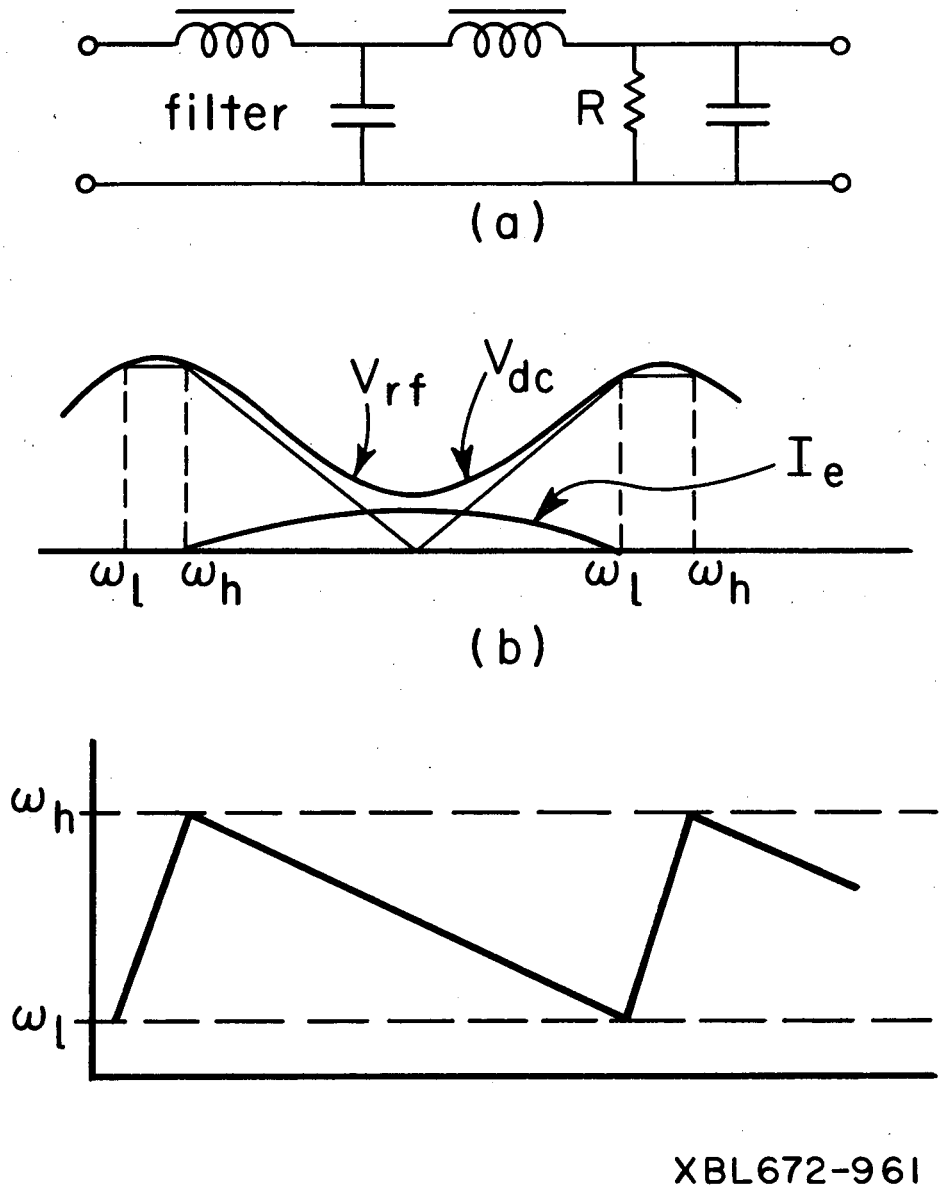

Figs. 15 and 16

TRANSMISSION LINE EFFECTS

Identical Circuits

So far we have neglected the fact that the inductances are really usually sections of transmission lines. Some energy is stored in the distributed capacity of these lines, which results in an increase of the total stored electrostatic energy. In a manner similar to the extra emission required by the capacitively coupled system, we would expect transmission-line effects to require an increase in the electron-emission current for a given required frequency swing. It remains to determine the magnitude of this effect.

When the lines are short ($<<\lambda/4$), the inductance is proportional to the length of the line and the distributed capacity can be neglected. Figure 17 shows this case. The antisymmetric mode frequency is proportional to $(xC)^{-1/2}$. The coupling inductance is assumed to be a short section of line Δx, with the same Z_o. Figure 17(b) shows this element split into two parts, each with twice the inductance and twice the length, $2\Delta x$. The symmetric mode frequency is proportional to $[C(x+2\Delta x)]^{-1/2} \approx [1-(\Delta x/x)](xC)^{-1/2}$. The frequency interval between modes is therefore given by

$$\Delta\omega/\omega \approx \Delta x/x, \tag{42}$$

and is to be compared with the relation $\Delta\omega/\omega = M/L$ as given in Eq. (17).

When the lines are long enough to be self-resonant, (i.e., $C = 0$), the situation is as shown in Fig. 18. Here we see at once

$$\Delta\omega/\omega = 2\,\Delta x/x. \tag{43}$$

The intermediate case is shown in Fig. 19, where $x < \lambda/4$. The Z_o of the line is determined from the relation $1/\omega_h C = Z_o \tan(\omega_h/c)x$, where ω_h is the higher-symmetric-mode frequency, and c is the velocity of light. At the lower mode frequency, we have

$$1/\omega_h C = \frac{1}{\omega_h C \tan\frac{\omega_h}{c}x} \tan\frac{\omega_\ell}{c}(x+2\Delta x),$$

or

$$\frac{\omega_\ell}{c}(x+2\Delta x) = \tan^{-1}\left(\frac{\omega_h}{\omega_\ell}\tan\frac{\omega_h}{c}x\right) = \tan^{-1}\left[\left(1+\frac{\Delta\omega}{\omega}\right)\tan\frac{\omega_h}{c}x\right]$$

$$= \tan^{-1}\left[\tan\frac{\omega_h}{c}x + \frac{\Delta\omega}{\omega}\tan\frac{\omega_h}{c}x\right].$$

For $\Delta\omega/\omega<<1$ we can expand in the vicinity of $\tan^{-1}\tan\frac{\omega_h}{c}x$:

$$\frac{\omega_\ell}{c}(x+2\Delta x) = \tan^{-1}\left(\tan\frac{\omega_h}{c}x\right) + \tan^{-1}\left(\frac{\Delta\omega}{\omega}\sin\frac{\omega_h}{c}x\cos\frac{\omega_h}{c}x\right) = \frac{\omega_h}{c}x + \frac{\Delta\omega}{\omega}\sin\frac{\omega_h}{c}x\cos\frac{\omega_h}{c}x. \tag{44}$$

If we write $\omega_h/\omega_\ell = 1+(\Delta\omega/\omega)$, and solve for $\Delta x/x$, we have

$$\frac{\Delta x}{x} = \frac{1}{2}\left(1+\frac{c}{\omega x}\sin\frac{\omega x}{c}\cos\frac{\omega x}{c}\frac{\Delta\omega}{\omega}\right). \tag{45}$$

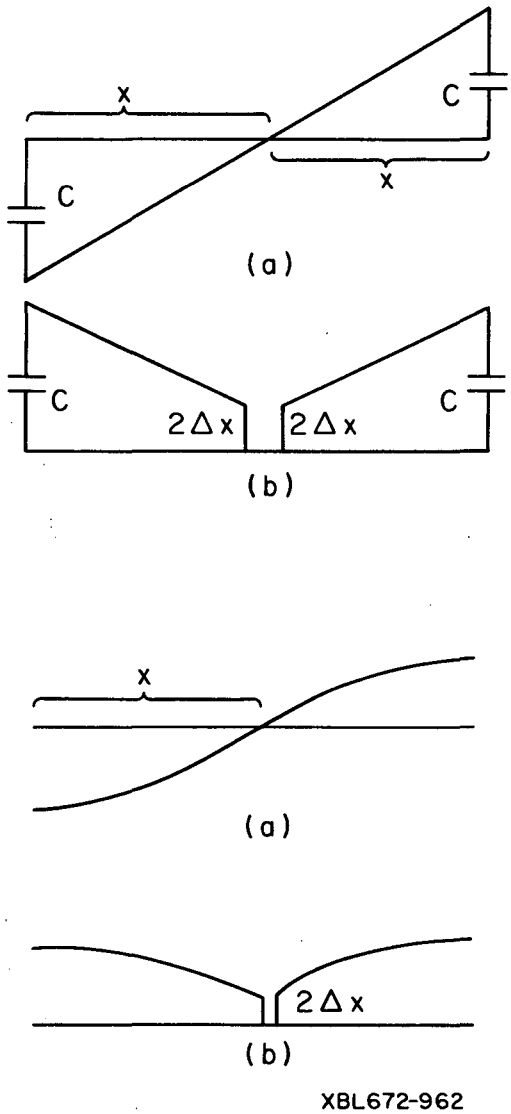

Figs. 17 and 18

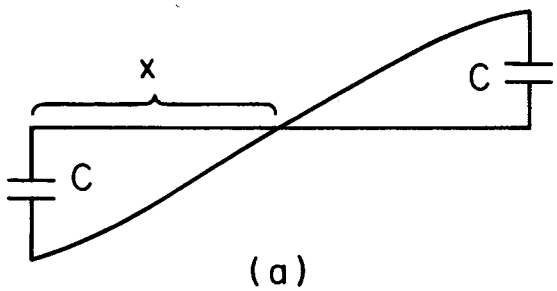

(a)

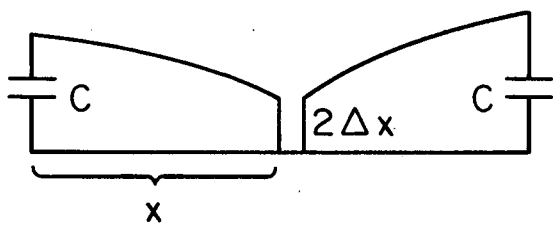

(b)

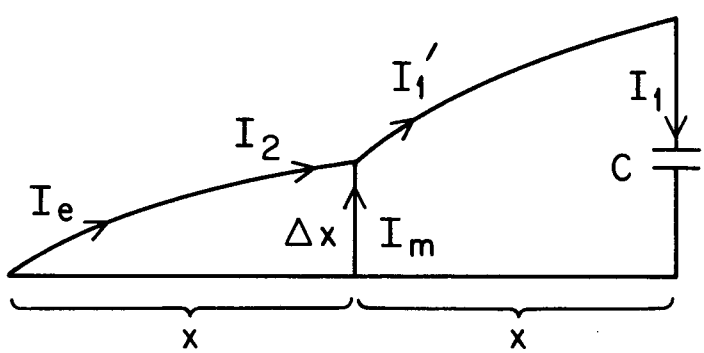

XBL672-963

Figs. 19 and 20

As we saw earlier, the electron current I_e maximizes at series resonance. Figure 20 shows this situation. Currents I_2 and I_m are determined by their respective line impedances:

$$\frac{I_2}{I_m} = \frac{Z_o \tan 2\pi\Delta x/\lambda}{Z_o \tan 2\pi x/\lambda} \approx I_2/I_1', \tag{46}$$

since

$$\Delta x/x << 1; \quad I_1' = I_1/(\cos 2\pi x/\lambda); \quad \text{and} \quad I_2 = I_c \cos 2\pi x/\lambda .$$

Inserting in Eq. (46), we have:

$$I_e = I_1 \left(\frac{2\pi\Delta x}{\lambda}\right)/\left[\sin\left(\frac{2\pi x}{\lambda}\right) \cos\left(\frac{2\pi x}{\lambda}\right)\right].$$

If we let $\theta = 2\pi x/\lambda$, the equation becomes

$$I_e = \theta I_1(\Delta x/x)/\sin\theta \cos\theta. \tag{47}$$

Substituting the value of $\Delta x/x$ from Eq. (45), and putting $\omega x/c = \theta$ and $I_1 = V_1 C_1 \omega$, we have

$$I_e = \frac{1}{2}\left\{\frac{\theta}{\sin\theta\cos\theta} + 1\right\} V_1 C\Delta\omega = k\, V_1 C\Delta\omega. \tag{48}$$

Figure 21 shows k plotted against the line length θ. The graph shows that lines in excess of $\lambda/8$ rapidly become very costly in terms of required emission and power.

Accelerating Electrode as a Transmission Line

However, not all line effects are bad. The capacity C_1 may represent an appreciable fraction of a wavelength, such as in the case of the center-fed "C" electrodes for a cyclotron mentioned in the introduction. Then C_1 becomes the capacity looking into an open-ended transmission line and is somewhat greater than the dc capacity of the electrode. It also changes with frequency, so that the ratio V_1/V_2 will be different at ω_h and ω_ℓ. On the other hand, there will be a voltage step-up along the line. While the line is short, these factors do not have much effect on the previous analysis.

If the electrode represents a long line such as a 180-deg center-fed "C" electrode in a large cyclotron, then the line effects predominate, and we must consider the extreme case. In Fig. 22(a) the electrode of length x_1 and impedance Z_o is assumed to look like $\lambda/4$ at ω_h. To start with some symmetry in the problem, we assume that the line of length x_2 has the same Z_o, and the node is located at the mutual element of length Δx (also with impedance Z_o).

At ω_ℓ (Fig. 22(b)), the mutual element divides so that

$$1/\Delta x_1 + 1/\Delta x_2 = 1/\Delta x . \tag{49}$$

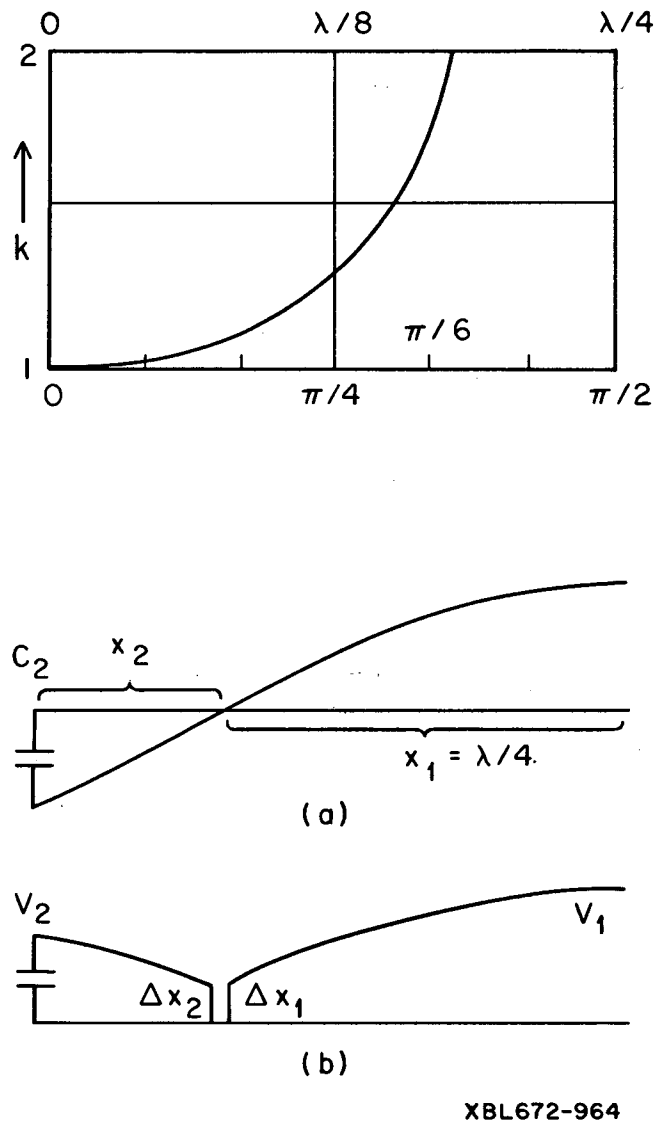

Figs. 21 and 22

Keeping in mind the bad effects of long lines when we are dealing with lumped capacities (Fig. 21), we will make x_2 as short as possible. Then, using the relations in Eqs. (42) and (43), we find

$$\Delta\omega/\omega = \Delta x_1/x = 2\Delta x_2/x_2 \,. \tag{50}$$

Combining Eqs. (49) and (50), we have

$$\Delta x = \Delta x_2/[1+(2x_2/x_1)] \,. \tag{51}$$

At series resonance the voltage distribution is as shown as in Fig. 23. As before, we write

$$I_e/I_m \approx I_e/I_1 = \Delta x/x_2 \,.$$

Substituting for Δx from (51), we write

$$I_e = I_1(\Delta x_2/x_2)/(1+2x_2/x_1) = I_1(2\Delta\omega/\omega)/(1+2x_2/x_1).$$

Since x_1 is still approximately $\lambda/4$ at series resonance, we can write

$$I_e = \left(\frac{V_1}{Z_o}\right)\left(\frac{2\Delta\omega}{\omega}\right)\frac{1}{[(1+(2x_2/x_1)]} \,. \tag{52}$$

Replacing $1/Z_o\omega$ by $C_2 \tan 2\pi x_2/\lambda$, and $1/\lambda$ by $1/4x_1$ yields

$$I_e = 2V_1C_2 \frac{\tan(\pi x_2/2x_1)}{1+2x_2/x_1}\Delta\omega \,. \tag{53}$$

If we put $x_2 = \lambda/8 = \frac{1}{2}x_1$, which can easily occur in practice, we find

$$I_e = V_1C_2\Delta\omega. \tag{54}$$

This is the same relation we found in Eq. (18), since we had assumed that $C_2 = C_1$.

If we let $x_2 = \frac{1}{2}x_1 + \delta$ and expand the tangent, Eq. (53) becomes

$$I_e = V_1C_2\Delta\omega\left[\frac{1+(\pi/4)(\delta/x_1)}{1+\delta/x_1}\right] \,. \tag{55}$$

Since we have $\pi/4\,\delta \approx \delta$, Eq. (34) shows that for a reasonable range in the neighborhood of $x_2 = \lambda/4$ the required emission is essentially given by Eq. (54). As δ is made progressively negative, the emission decreases as long as the approximations are valid (obviously I_e must increase as δ approaches zero). The conclusion is that for a desired voltage V_1 over a range $\Delta\omega$, substitution of an open-ended line for the lumped circuit (1) does not increase the tube emission requirements. This statement must be qualified, however. Figure 21 shows that about 30% more emission is needed if two lumped circuits with $\lambda/8$ lines are used. With only one $\lambda/8$ line [in circuit (2)], we could guess that a 15% increase would result. On the other hand, we note that for this case we have $V_1 = \sqrt{2}\,V_2$ as shown in Fig. 22. Hence the increased emission is offset by a lower tube voltage and a saving in power.

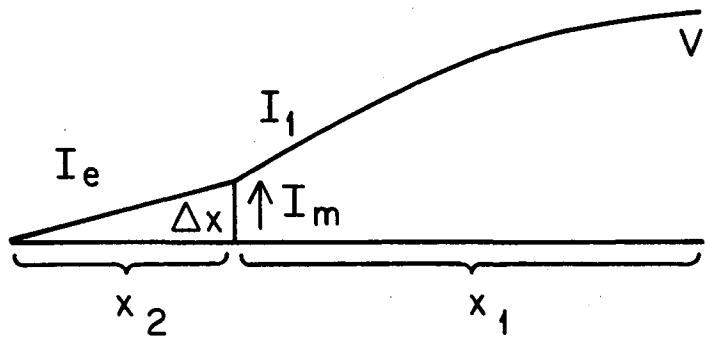

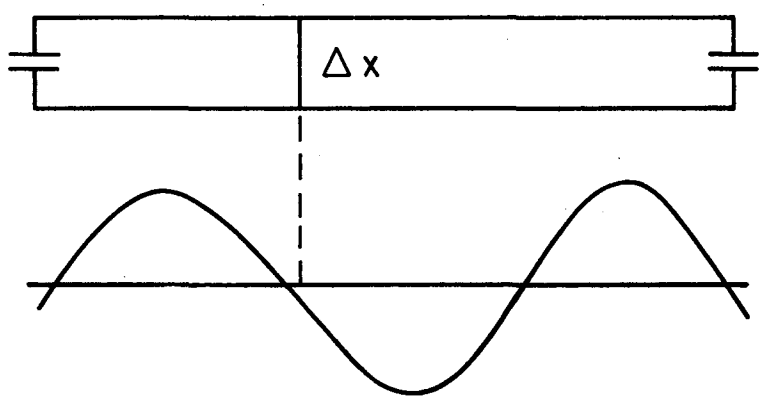

XBL672-965

Figs. 23 and 24

MODULATION RATES, HIGHER MODES, AND PARASITICS

Modulation Rates

Figure 15 shows a sawtooth modulation program with a finite fly-back time which we now examine. The fastest way to change from ω_ℓ to ω_h is to change the grid driving-frequency suddenly and increase the grid voltage to its maximum. The circuit is oscillating at ω_ℓ, but since the two modes are orthogonal, ω_h can build up independently. This can happen very rapidly, since the necessary size of the amplifier tube ensures plenty of emission to charge up C_1 and C_2. During each cycle a pulse of current flows whose average value is just I_{dc}. The time required is therefor $t = (C_1+C_2)V/I_{dc}$. For typical values, this time is of the order of microseconds.

Since we have assumed no losses, the circuit is now oscillating in both modes, and beats occur. For identical circuits all the energy will alternately transfer completely from one circuit to the other. The unwanted mode ω_ℓ must be removed by inserting losses such as a parallel resistor which will absorb power at all times, or by an auxiliary gated triode which could be turned on when needed. The latter would, however, add capacity and reduce the frequency range. If two amplifier tubes are used, one can build up ω_h while the other absorbs ω_ℓ, and then both can act in parallel to produce the much slower frequency program.

In practice such complications would seldom be necessary, since simple resistor damping, with a decay rate several times longer than the build-up time, is usually adequate. This resistor should be placed in circuit (2) (if only the range $\Delta\omega$ is to be used), since it absorbs very little power near series resonance when the emission demands are greatest. On the other hand, if the full possible range 1.4 $\Delta\omega$ is to be used, the resistor should be in circuit (1).

The resistor serves another purpose since the above-mode damping process occurs continually throughout the normal modulation program. To see this, we imagine that C_2 is a mechanical variable capacitor which can be changed instantly during one cycle. When C_1 and C_2 are charged to their peak voltage, we can imagine that C_2 is suddenly decreased. As a result V_2 suddenly increases, which we note is opposite to the change shown in Fig. 5(a) and contrary to the voltage and resonance conditions of Eq. (11) and (12). The reason for this is that a transient has been generated. We now have a mixture of the symmetric and antisymmetric mode with a phase relationship such that V_2 is increased. At slow modulation rates, normal losses obscure this effect. At high rates it might be noticeable without a damping resistor.

Higher Modes

Every physical circuit has an infinity of higher modes, and our coupled system with sections of line here and there can easily have several that will cause trouble. They have been given special attention in some rotating capacitor systems where the oscillator tube is not much bigger than necessary to overcome normal losses. In an electronic broadband system, the tube must be at least an order of magnitude larger than in a rotating-capacitor system, and the Fourier components of the current pulses will be correspondingly larger. Throughout the range $\Delta\omega$, every effort should be

made to prevent a higher mode of the system from coinciding with any of the first few harmonics of the current pulses. The wider the range $\Delta\omega$, the more difficult this becomes.

Figure 24 shows the nature of some of the higher modes. They usually have quite a high Q. The voltage maxima occur where the capacity is purposely minimized (to increase $\Delta\omega$), and the nodes occur very close to C_1 and C_2. The voltage step-up is therefore large, and it is easy to generate hundreds of kilovolts.

The higher modes can be detuned without appreciably affecting the main mode by placing small capacitors at the voltage maxima. It is almost impossible to dodge the very high modes, but fortunately they are excited weakly and can be damped by resistors across the lines. The resistors are also effective for the first few modes. For the most bothersome, a more elegant method is to couple a very lossy circuit tuned to the unwanted mode frequency. If critical coupling is employed, the Q can be reduced to the point where the voltage rise is not objectionable as the harmonic of the fundamental passes through the mode frequency. Even with all these precautions, the higher modes can cause trouble. Glow discharges in the associated vacuum portions of the system can change the higher-mode frequencies by many megacycles and cause overlaps that would otherwise not exist.

Parasitics

Isolation between the input circuit and the output is never completely perfect. Some slight coupling is always present, even in the best shield grid tubes (or triodes in a grounded-grid circuit), and this coupling can result in feedback that causes oscillation at unwanted higher frequencies, known as parasitics.

In contrast to the problem of coincidence of higher-order modes with harmonics of the fundamental, the parasitic problem is not accentuated by the high filament emission demanded by the nature of the broadband system. In fact, the high driving levels tend to swamp such unwanted frequencies. Nevertheless the grid driving circuit should be designed to avoid parasitic possibilities. One simple procedure is to make the circuit quite lossy, which is in line with the usual methods of making a broadband network. This should cause very little inconvenience, since the broadband problem in the driving circuit, with low voltages and low capacities is trivial compared with the problem in the high-Q output circuit.

ALTERNATIVE ARRANGEMENTS AND MULTI-CIRCUIT SYSTEMS

Coupling Variations

The inductive and capacitive coupling schemes shown in Fig. 3 and Fig. 13 respectively, are not the only possibilities. Figures 25 and 26 show alternative arrangements. Figure 25, (b) and (c) show the two modes that exist when point-to-point inductive coupling is used. In the antisymmetric mode, a node appears somewhere along L_m, and the two series inductances $L_a{}^a$ and $L_b{}^a$ add in parallel to their respective circuits to make them

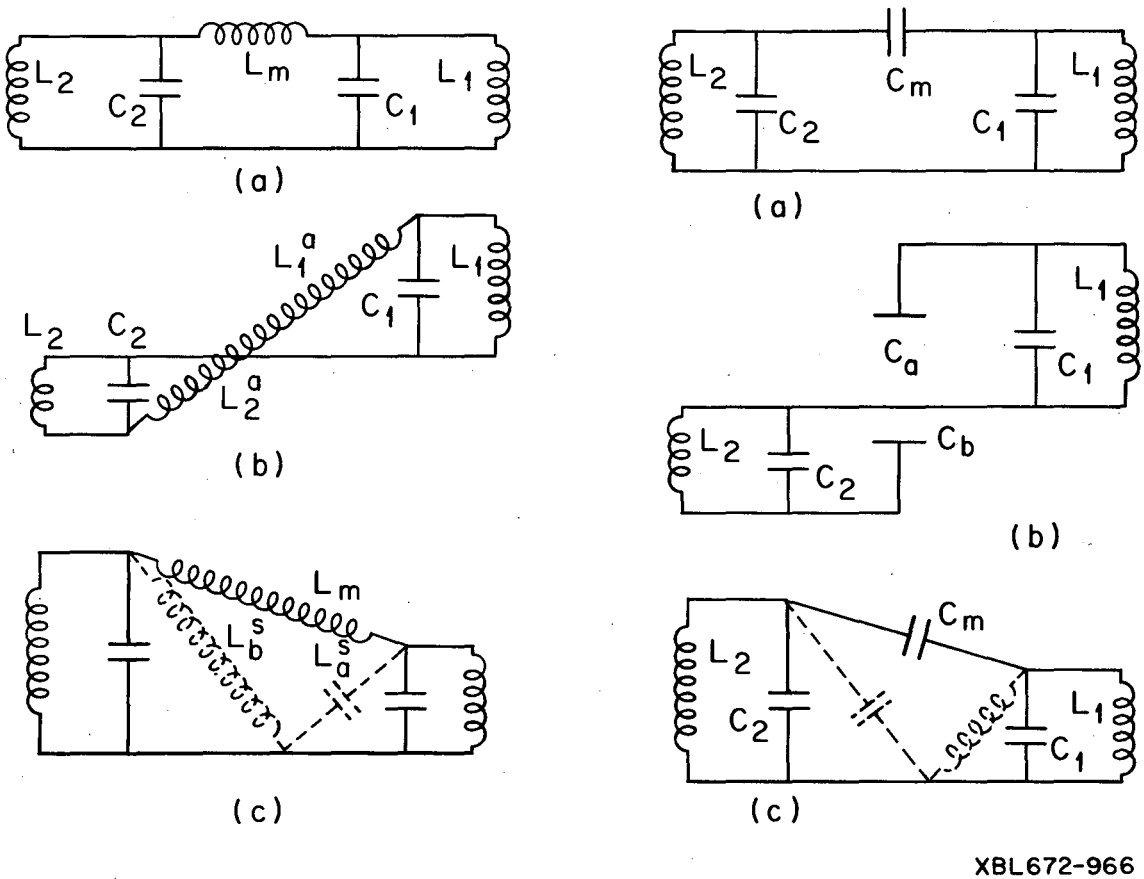

Figs. 25 and 26

resonate at the same frequency. We have

$$C_1 L_1 L_a^a/(L_1+L_a^a) = C_2 L_2 L_b^a/(L_2+L_o^a)$$

and $L_m = L_a^a + L_b^a$. A quadratic equation results; we solve for L_a^a and L_b^a, and obtain L_a^a, L_a^s, L_b^a, L_b^s, one of which will be negative. Figure 25 (c) shows L_m replaced by a series circuit with the common connection at ground potential. Again L_a^s and L_b^s add in parallel to their respective circuits to make both circuits resonate at the same frequency in the symmetric mode.

Figure 26, (b) and (c) show the same behavior for capacitive coupling. In the antisymmetric mode, a ground plane can be visualized somewhere between the plates of C_m. In the symmetric mode C_m is replaced by an equivalent series circuit with the common connection at ground.

These two arrangements are equivalent except at series resonance shown in Fig. 27. In the capacitively coupled case, Fig. 27(b), the tube emission current must charge up the capacity $C_m + C_1$, and therefore the maximum frequency range is less than possible with the circuit of Fig. 27(a). In spite of this factor (unknown at the time), the circuit of Fig. 26(a) was model-tested for the first fm cyclotron at Berkeley in 1946 and found to be hopelessly emission-limited in view of the required voltage and huge dee capacity. Further complications were also encountered. The required separation between the dee capacity C_1 and the tube meant that the leads to C_m were sizeable sections of transmission line with considerable inductance. The system then became a three-circuit arrangement with no benefit from the third circuit because of its series-resonant nature.

A somewhat similar disadvantage holds for the inductively coupled case in Fig. 25(a). Here L_m becomes a transmission line with parallel capacity to ground, and we have already observed the frequency-limiting results of adding extra capacity to ground.

When we physically separate C_1 and C_2 and are forced to add parallel stray capacity to L_m and series inductance to C_m, we are dealing with a sort of "matching section."

Multicircuit Systems

All matching sections except the simple transformer (Fig. 3, which we have treated extensively) involve capacities, and we can ask ourselves whether there is any way to introduce such extra capacity without reducing the possible frequency range. One rather obvious notion is to add any extra capacity in the form of a tube with enough emission to cancel at least its own bad effects.

The physical location of such a tube is subject to the same limitations as the amplifier tube, so the possible coupling arrangements are few. One possibility is shown in Fig. 28. One can imagine circuits (1) and (2) behaving as previously discussed with the filament emission of C_2 causing a smooth transfer from the symmetric to the antisymmetric mode. At the same time we can think of the emission of C_3 doing nothing but keeping V_3 in phase

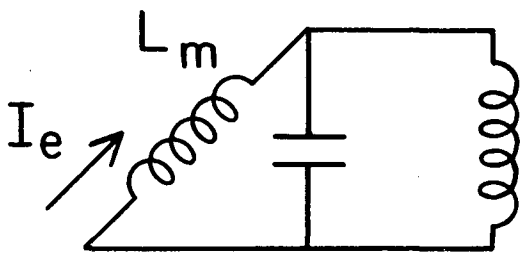

(a)

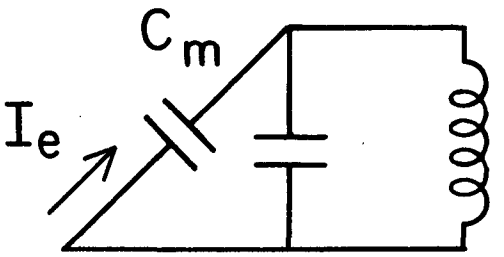

(b)

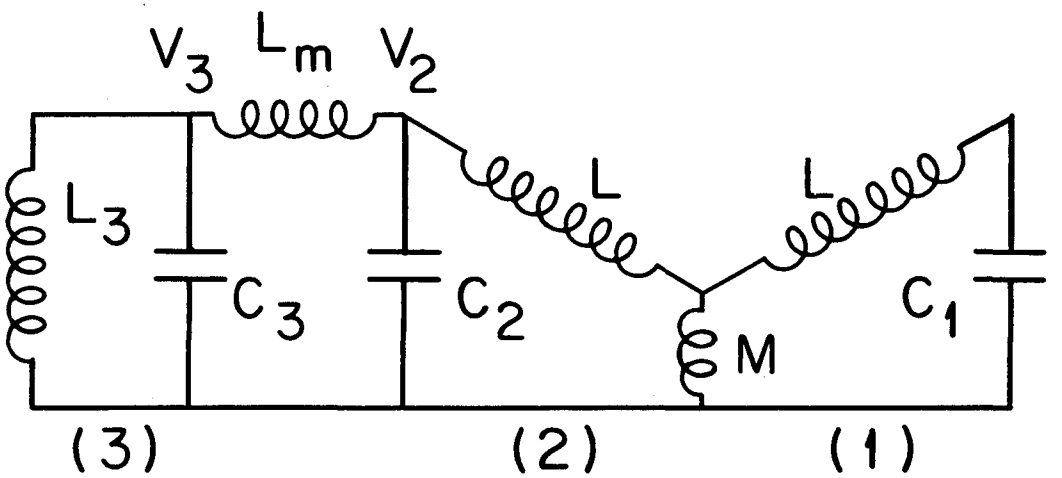

XBL672-967

Figs. 27 and 28

with V_2. Then at the upper frequency ω_h, extra emission could be used to raise the frequency still further, finally arriving at a third normal mode of the system shown in Fig. 29. The inductances $L_1{}^a$ and $L_2{}^a$ add in parallel to each side and raise the frequency above our former ω_h.

Unfortunately this is not possible in this simple arrangement since, as we saw earlier [Eq. (7)] the single circuit with the inherent tube capacity alone can just barely cover the double-circuit range $\Delta\omega$. However, another circuit can be added--the mirror image of Fig. 4, shown in Fig. 30(a), where C_2, C_3, and C_4 are tubes, and $C_4 = C_1$. With C_4 idling, the respective emission currents of C_2 and C_3 cause both mirror circuits to cover the range $\Delta\omega$, with V_2 and V_3 in phase. The emission of C_2, C_2 and C_4 is then used to raise the frequency still farther, put V_2 and V_3 out of phase, and reach the higher normal mode shown in Fig. 30(b). At this frequency the emission current in all three tubes again becomes zero except for circuit losses. The benefit is seen to be small, since the inductances $1/2\ L_m$ must raise the frequency of both double-tuned circuits, and the effect is primarily to raise the voltages of the nearby capacities C_2 and C_3.

The concept can be extended by adding further double-tuned circuits in chain fashion, with rapidly decreasing effectiveness. As other authors[4,6] have concluded, the advantage over two circuits is not worth the complication. The problem of the multiplicity of higher-order modes with the attendant possibility of momentary excessive voltages, plus the parasitic possibilities due to numerous stray capacity feedback paths, make such complex circuits decidedly unattractive.

AVERAGE POWER AND POWER-SUPPLY DESIGN

Average Power

Figure 6 shows the tube rf voltage V_2 throughout the total possible range $1.4\ \Delta\omega$. With a constant dc plate voltage and a constant rf voltage, V_1 is approximately $0.7\ V_{2(max)}$. Figure 31 shows the tube rf voltage V_2, and the power P (which is proportional to $|I_e|$). We assume that V_{dc} is $1.2\ V_{2(max)}$, in order to obtain full 180-deg flow at the extremes.

From Eq. (15), we have $I_e = (M_1/M)[2-(M_1/M)][M/(L+M_1)]\,V_1 C_1\,\omega$. If we neglect M_1 compared with L, put $M/L = \Delta\omega/\omega$ (from Eq. 17), and let $M_1/M = x$, we have $|I_e| = |x(2-x)|\,V_1 C_1 \Delta\omega$. At any point within the range, we have

$$P = I_{dc}V_{dc} \approx (1.2)(0.6|I_e|)V_2 = (1.2)(0.6|I_e|)(1.4)V_1 \approx I_e V_1 = |x(2-x)|\,V_1{}^2 C\Delta\omega. \tag{56}$$

The average power can be written

$$\overline{P} = (V_1{}^2 C\Delta\omega)\,\frac{\int_{-0.4}^{0}|x(2-x)dx + \int_0^1 |x(2-x)|\,dx}{1.4},$$

or

$$\overline{P} = 0.56\ V_1{}^2\ C\Delta\omega, \tag{57}$$

where $\Delta\omega$ is the separation between modes, and the total range is $1.4\ \Delta\omega$.

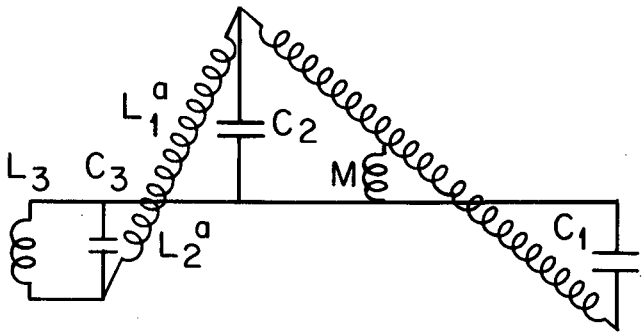

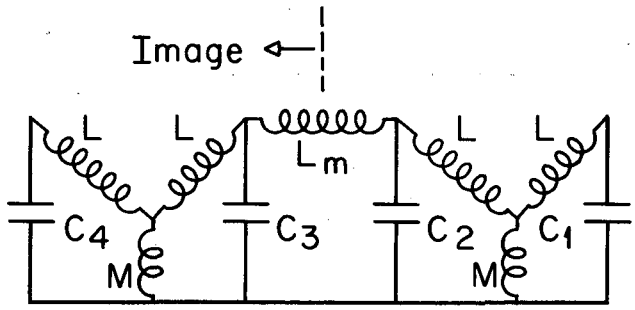

(a)

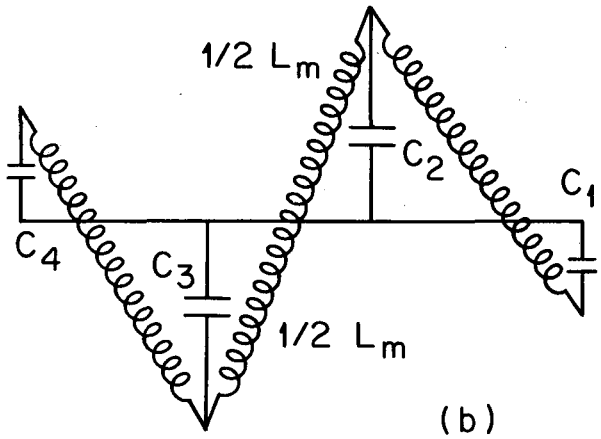

(b)

XBL672-968

Figs. 29 and 30

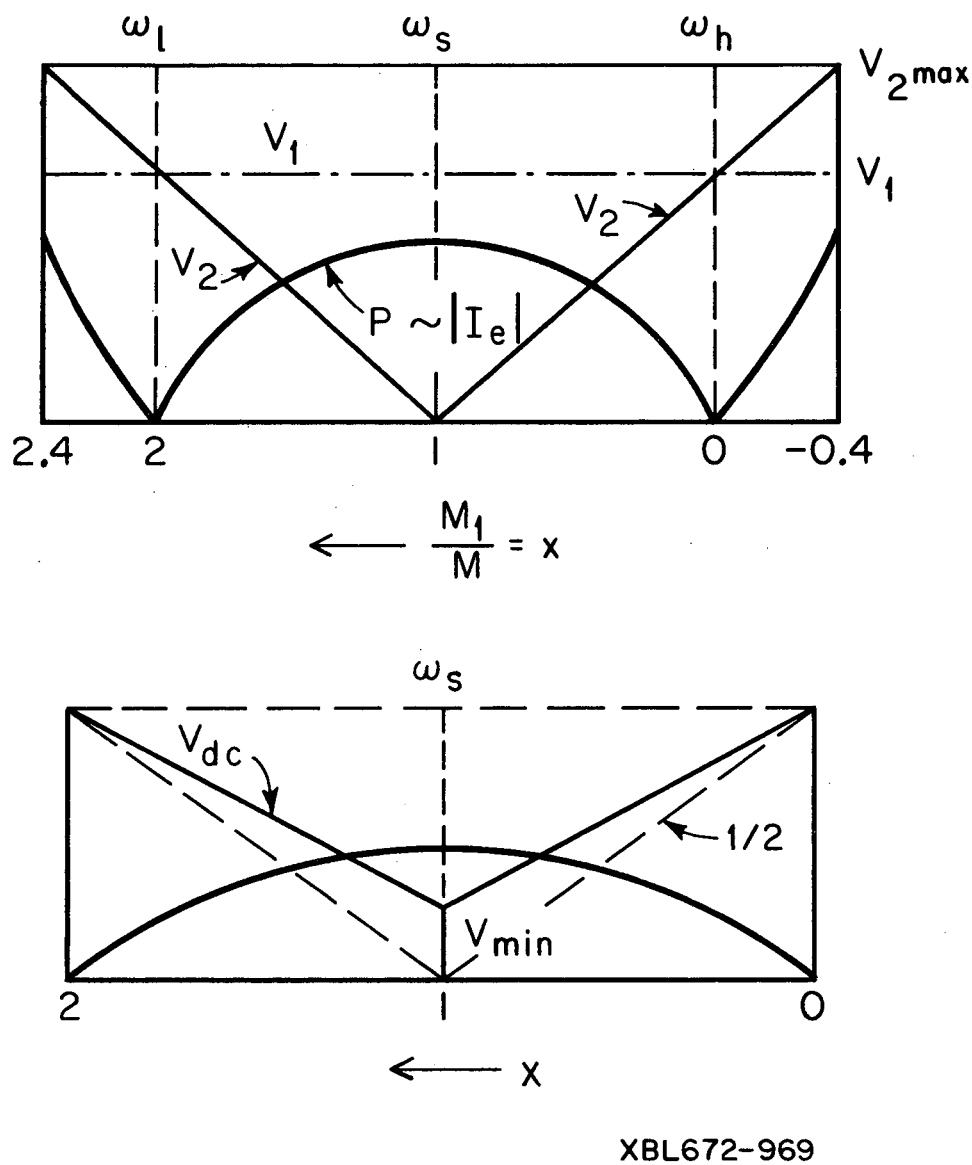

XBL672-969

Figs. 31 and 32

If only the range $\Delta\omega$ is considered, we have $V_2 = V_1$ instead of $1.4\ V_1$, and we can let $V_{dc} = V_2$ (instead of $1.2\ V_2$). (Actually we could let V_{dc} be somewhat less than V_2, since, as noted by Fiebig,[4] very little current is needed near ω_ℓ and ω_h, and the angle of flow can be much less than 180 deg. We have, therefore,

$$\overline{P} = \frac{1}{1.2}\ \frac{V_1^2}{1.4}\ C_1 \Delta\omega \int_0^1 |x(2-x)|\,dx = 0.4\ V_1^2\ C_1 \Delta\omega. \tag{58}$$

If V_{dc} is now programmed so that $V_{dc} = V_{2(max)}$ at ω_ℓ and ω_h and $V_{dc(min)} = R\,V_{2(max)}$ at ω_s, a further reduction can be realized. Figure 32 shows this case. For $1>x>0$, we have $I_e \sim \frac{M_1}{M}(2-\frac{M_1}{M}) = Kx(2-x)$ and $V_{dc} = (1-x)\ V_{max} + x R\ V_{max} = V_{max}(1-x+R)$. The power ratio is

$$\frac{\overline{P}(V_{dc}\ \text{program})}{\overline{P}(V_{dc}\ \text{constant})} = \frac{K V_{max} \int_0^1 x(2-x)(1-x+xR)dc}{K\ V_{max} \int_0^1 x\,(2-x)\ dx} = (3+5R)/8. \tag{59}$$

If we take $V_{2(min)}/V_{2(max)} = 1/5$ as a realistic ratio, we have

$$\frac{\overline{P}(\text{programmed})\ V_{dc})}{\overline{P}(\text{constant} + V_{dc})} = \frac{1}{2}\ .$$

Thus for this case we have

$$\overline{P} \approx (0.2)\ V_1^2\ C_1\ \Delta\omega. \tag{60}$$

Power Supply Design

As shown in Fig. 15, a resonant choke can approximate the desired variation in V_2. As the frequency is varied at some repetition rate, the plate-current pulses shown in Fig. 32 drive the LC circuit at the repetition rate. The oscillations are damped by the resistor R, which unfortunately will dissipate the same power as the modulator tube (after a steady state is reached).

Figure 33 shows one way in which the stored energy can be fed back to the supply. C_f is the supply filter capacitor. L and C are resonant at the fm frequency. T_2 is a winding such that $T_1/T_2 = (V-V_{min})/V$. When the oscillation builds up to the value shown in Fig. 33, the diode conducts; charge is fed back to the supply, and the oscillation level is automatically clipped and regulated at the proper level. The loading is resistive so the inductance of T_2 enters only as a correction factor. The current i_2 also tends to unsaturate the core, which makes the choke L much smaller. From the diagram $V_{2(max)}$ is almost twice the supply voltage V. In most cases, the ratio will be approximately $\sqrt{3}$, which is the change that is effected by reconnecting the transformer from Y to Δ.

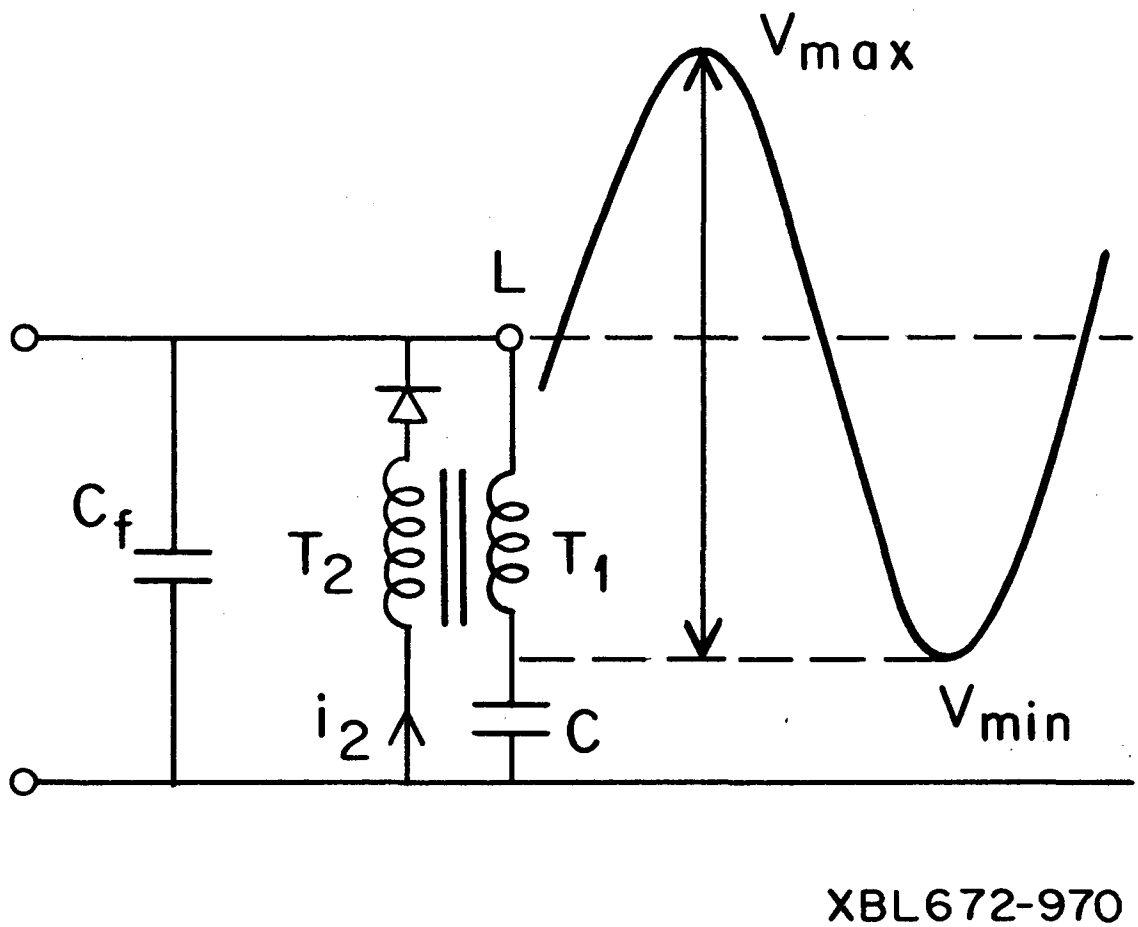

Fig. 33

DISCUSSION AND NUMERICAL EXAMPLE

Summary

Perhaps the most pertinent aspect of the foregoing analysis is the emphasis on minimizing transmission-line effects. Where the accelerating electrode is itself a section of line and only the voltage along an edge is important, the rise in voltage along the line partially offsets the bad effects of stray capacity. However, in this case the impedance should still be as high as possible to minimize such distributed capacity. In all other portions of the circuit, stray capacities and distributed line capacities should be as small as possible, which in turn means that all lines should be as short as possible.

The inherent capacity of the amplifier tubes is unavoidable, but care must be taken to minimize stray anode-to-ground capacity. Tubes with the anode inside the filament structure make this design problem less difficult and are an obvious choice, provided that the g factor is adequate ($g = I_e/C$, where C includes stray capacity).

The frequency range for the two-circuit arrangement is governed by the relations $V\Delta\omega = g$ for identical circuits, and $V\Delta\omega = \gamma g$ for nonidentical circuits, where γ is the ratio of electrode to tube voltage in both normal modes of the system, and $\Delta\omega$ is the separation between modes. (Although not considered here, a more complex relation can be derived where γ has different values at the two mode frequencies). The maximum possible range permitted by filament emission is given by $V\Delta\omega = (1.4)\,\gamma g$.

The most interesting aspect of these formulae is the fact that the accelerating electrode capacity does not enter explicitly. The voltage bandwidth product depends only on the tube characteristics and our choice of the voltage ratio γ. The total tube capacity is related to the electrode capacity through the relation $C_2 = \gamma^2 C_1$, and this in turn determines the number of tubes required. The factors that enter into the choice of γ are (1) the frequency range limitation $V\Delta\omega = \gamma g$, which demands that γ be large; (2) the geometric limitation on the frequency range[Eq. (31)] which depends only on the coupling arrangement $\omega_h^2/\omega_\ell^2 = (\gamma+1)(\beta-\gamma)/(\gamma-1)(\beta+1)$ and demands that γ be small; (3) the correction for line effects, which introduces a factor k (Fig. 21); and (4) the requirement that the tube operate within its voltage rating, which will usually limit V_2 to something below 20 kV.

After an arrangement has been found that gives the desired voltage-bandwidth product, the power requirements must be settled. If the available emission is marginal, so that $V\Delta\omega = 1.4\,\gamma g$, the minimum power with constant V_{dc} will be approximately given by Eq. (57). If there is room to add more tubes in parallel (thus increasing γ), there will be emission to spare and the range can be reached by increasing the mode separation. The relation is then $V\Delta\omega = \gamma g$, and if constant dc voltage is used, the power is given by Eq. (58). Finally, if a programmed dc supply is used, the power is given by Eq. (60).

It should be emphasized that, where the electrode capacity C_1 and the tube capacity C_2 are the only capacities in the system, the simple overcoupled transformer is probably the best circuit to use for electronic frequency modulation. A slightly greater range can be achieved by adding images of this circuit, but only at the expense of great complexity and probable troubles in the form of a multiplicity of unwanted modes, spurious high voltages, sparks, and other mysterious troubles.

The resonator need not be of the type peculiar to cyclotrons, but can have any shape. If it is a cavity, loop coupling will provide the mutual element, and the ratio M/L will be approximately replaced by the ratio of cavity flux linking the loop to the total cavity flux. L_2 then includes most of the loop inductance. Since L_2 has been shown to be much smaller than L_1 for best performance, it follows that the modulating tube (or tubes) will be very close to the cavity. The tube should be close in any case to minimize line effects. The usual presence of dc magnetic fields presents a problem when the tubes are placed as close as possible to the resonator. If the anodes are small in diameter (as they usually are with water-cooled tubes) a lot can be accomplished with cylindrical iron shields without unduly increasing stray capacity to ground. Air-cooled tubes with large radiators are to be avoided due to higher inherent stray capacity and reduced effectiveness of the larger diameter magnetic shields.

Numerical Example

Let the requirements be 25 kV peak on an electrode of capacity 100 pf. Let us use a tube with a plate-to-ground capacity of 100 pf and a dc current of 20 A that operates comfortably at 12.5 kV dc (and 12.5 kV peak rf at both normal mode frequencies). At a flow angle of 180 deg, the peak rf current will be approximately 33 A. Therefore we have $g = 1/3\times10^{12}$ AF and $\gamma = 2$. The frequency range is $\Delta f = \Delta\omega/2\pi = \gamma g/2\pi V_1 \approx 4$ Mc. Since we have $C_2 = \gamma^2 C_1$, four such tubes are required to cover this range.

Although the range $\Delta\omega$ is independent of the nominal frequency, the ratio M/L is not. For identical circuits we can write $\Delta\omega/\omega \approx M/L$. For nonidentical circuits we use Eq. (32): $\Delta\omega/\omega = (\beta-\gamma^2)/\gamma(\gamma^2-1)$, or the exact relation, Eq. (31): $\omega_h^2/\omega_\ell^2 = (\gamma+1)(\beta-\gamma)/(\gamma-1)(\beta-\gamma)$. If we assume the range is 24 to 20 Mc and substitute in Eq. (31) with $\gamma = 2$, we find $\beta = L_1/L_2 = 5.7$. The inductance L_2 is therefore very small compared with L_1, and transmission-line effects can be neglected for this half of the circuit. If we assume that $L_1 \approx \lambda/8 \approx 2$ meters (which may be too short for many applications) then $L_2 = 40$ cm, which, for the size of tube we assumed, is of the order of the length of the anode. In terms of hardware, L_2 would be essentially the shortest connection that could be made between the tube and the mutual inductance M. From Eq. (29), $M = [1-(\gamma^2/\beta)]\, L_1/(\gamma^2-1) \approx L_1/10 \approx \lambda/80$, if M has the same Z_o as L_1.

The correction for line effects is found from Fig. 21, where we see that approximately 30% more emission is needed for a $\lambda/8$ line in both circuits. Since we have such a line in only one circuit, the correction is 15%, and Eq. (48) shows that, with the emission at maximum, the frequency range is reduced proportionately. Comparing Eq. (48) with Eq. (33), we see that the factors k and γ show up in the same manner, and therefore γ could be increased to compensate for such line effects as shown in Eq. (34). But in a

practical sense, we are already in some difficulty with $\gamma = 2$, since the length of the anode is already a sizeable fraction of the allowed value for L_2. In fact if L_2 is set equal to zero, Eq. (31) shows that $\gamma = 5$ is the maximum value we can use to cover the 24 to 20-Mc range.

The power is affected by the choice of γ only in that $\Delta\omega$ depends on γ. Using a programmed-dc-voltage approach (Fig. 31), the average power is found from Eq. (60) to be approximately 350 kW.

If γ is chosen as $\sqrt{2}$, the range becomes $4/\sqrt{2}$ Mc = 2.8 Mc. From Eq. (31) we have $\beta \approx 2.3$, so $L_2 = L_1/2.3$, which moves the tube considerably farther from M and possible dc magnetic fields. From Eq. (60) the power with programmed dc is approximately 210 kW. Since we have $\gamma = \sqrt{2}$ and $C_2 = \gamma^2 C_1$, we now need only two tubes in parallel. If we can possibly reduce stray capacities so that each tube has a plate-to-ground capacity of around 70 pf, we can put three tubes in parallel and have some 30% extra emission for transmission-line effects. From Fig. 21 we see that lines $\lambda/6$ in length require a 70% increase in emission. Since we need worry about only the one line L_1, we might make it of length $\lambda/6$ (requiring half the 70% extra shown in Fig. 21). The power is of course increased by some 35%, so we find an average power of approximately 300 kW for this case.

Figure 34 shows how such an arrangement might look. The division into three separate lines might be desirable or not, depending on geometrical aspects of the accelerator. However this arrangement emphasizes the reason why the range $\Delta\omega$ does not depend on C_1. If C_1 is doubled we merely double the number of tubes and lines. Damping resistors are shown halfway along L_2 to absorb higher-mode energy. The first higher mode of such a system has a half-wavelength approximately equal to the length of L_1 and presents a very low impedance at the tube. As the frequency rises, we find a mode where the length of $L_2 \approx \lambda/2$. This mode is heavily damped by the resistors. Resistors are also shown between tubes. They damp possible cross modes due to differences in tube performance.

The programmed dc-voltage method, coupled with a programmed grid drive probably makes the assumed feedback link unnecessary, unless precise voltage control of V_1 is needed. At ω_h and ω_ℓ the grid drive must be reduced to prevent the rf voltages V_1 and V_2 from greatly exceeding V_{dc}. The damping resistors to ground also help to limit V_1 and V_2 at ω_h and ω_ℓ, and are very effective if they have a low resistance. However, this means excessive extra power loss, and so their resistance should be no lower than necessary.

Finally, we can see from Fig. 34 why the fundamental limitation on the frequency range is determined only by the tube g factor and the tube voltage V_2, as shown by Eq. (35). Suppose we use a multiplicity of tubes and connect each to a section of line L_2 whose value will be assumed to be the same as shown in Fig. 34. As shown in Fig. 35, we now connect a multiplicity of very-high-impedance lines between L_2 and C_1 so that the total parallel inductance is the same as before even though L_1^1 goes to ∞ as n approaches ∞. The capacity C_1 is now made up of nC_1^1, where C_1^1 goes to 0 as n approaches ∞. We have $\gamma^2 = C_2^1/C_1^1$, and so γ approaches ∞ as C_1^1 goes to 0, since C_2^1 is the constant tube capacity. The voltage ratio $\gamma = V_1/V_2$ also

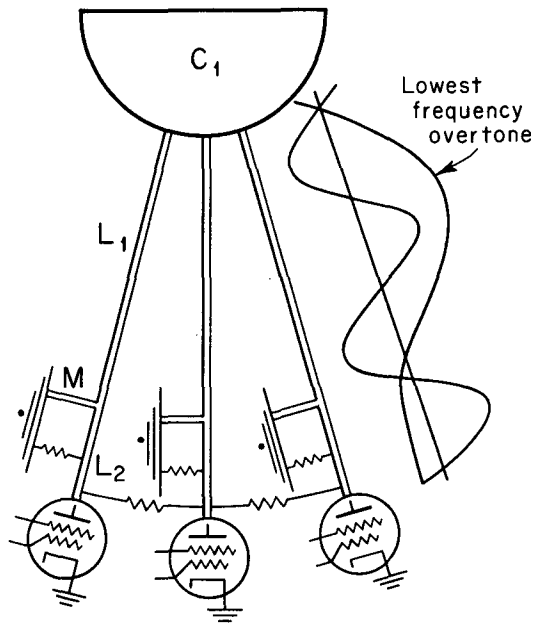

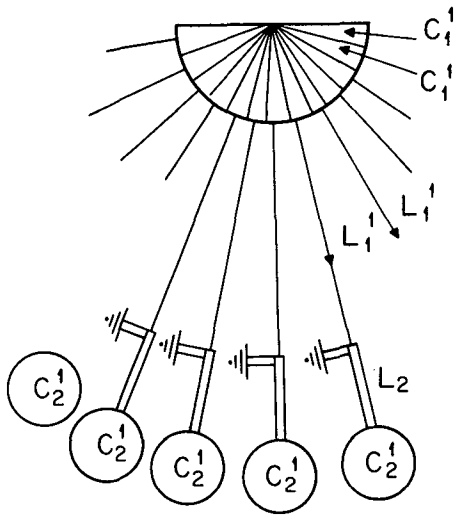

XBL672-971

Figs. 34 and 35

goes to ∞ as n approaches ∞. Therefore we see that neither the electrode capacity nor the required voltage impose a fundamental limitation on the frequency range, which is determined only by V_2 and g. Evidently V_2 should be as low as possible.

This report was prepared as an account of Government sponsored work. Neither the United States, nor the Commission, nor any person acting on behalf of the Commission:

A. Makes any warranty or representation, expressed or implied, with respect to the accuracy, completeness, or usefulness of the information contained in this report, or that the use of any information, apparatus, method, or process disclosed in this report may not infringe privately owned rights; or

B. Assumes any liabilities with respect to the use of, or for damages resulting from the use of any information, apparatus, method, or process disclosed in this report.

As used in the above, "person acting on behalf of the Commission" includes any employee or contractor of the Commission, or employee of such contractor, to the extent that such employee or contractor of the Commission, or employee of such contractor prepares, disseminates, or provides access to, any information pursuant to his employment or contract with the Commission, or his employment with such contractor.